AD_____

Award Number: W81XWH-05-1-0505

TITLE: Chemosensitization of breast cancer cells to chemotherapeutic agents by 3,3'-diindolylmethane (DIM)

PRINCIPAL INVESTIGATOR: KM Wahidur Rahman, Ph.D.

CONTRACTING ORGANIZATION: Wayne State University
                          Detroit, MI 48201-1928

REPORT DATE: August 2006

TYPE OF REPORT: Annual

PREPARED FOR: U.S. Army Medical Research and Materiel Command
               Fort Detrick, Maryland 21702-5012

REPORT DOCUMENTATION PAGE

Form Approved
OMB No. 0704-0188

Public reporting burden for this collection of information is estimated to average 1 hour per response, including the time for reviewing instructions, searching existing data sources, gathering and maintaining the data needed, and completing and reviewing this collection of information. Send comments regarding this burden estimate or any other aspect of this collection of information, including suggestions for reducing this burden to Department of Defense, Washington Headquarters Services, Directorate for Information Operations and Reports (0704-0188), 1215 Jefferson Davis Highway, Suite 1204, Arlington, VA 22202-4302. Respondents should be aware that notwithstanding any other provision of law, no person shall be subject to any penalty for failing to comply with a collection of information if it does not display a currently valid OMB control number. **PLEASE DO NOT RETURN YOUR FORM TO THE ABOVE ADDRESS.**

1. REPORT DATE *(DD-MM-YYYY)* 01/08/06	2. REPORT TYPE Annual	3. DATES COVERED *(From - To)* 25 Jul 2005 – 24 Jul 2006

4. TITLE AND SUBTITLE

Chemosensitization of breast cancer cells to chemotherapeutic agents by 3,3'-diindolylmethane (DIM)

5a. CONTRACT NUMBER

5b. GRANT NUMBER
W81XWH-05-1-0505

5c. PROGRAM ELEMENT NUMBER

6. AUTHOR(S)
KM Wahidur Rahman, Ph.D.

E-Mail: kmrahman@med.wayne.edu

5d. PROJECT NUMBER

5e. TASK NUMBER

5f. WORK UNIT NUMBER

7. PERFORMING ORGANIZATION NAME(S) AND ADDRESS(ES)

Wayne State University
Detroit, MI 48201-1928

8. PERFORMING ORGANIZATION REPORT NUMBER

9. SPONSORING / MONITORING AGENCY NAME(S) AND ADDRESS(ES)
U.S. Army Medical Research and Materiel Command
Fort Detrick, Maryland 21702-5012

10. SPONSOR/MONITOR'S ACRONYM(S)

11. SPONSOR/MONITOR'S REPORT NUMBER(S)

12. DISTRIBUTION / AVAILABILITY STATEMENT
Approved for Public Release; Distribution Unlimited

13. SUPPLEMENTARY NOTES

14. ABSTRACT: Constitutive activation of Akt or NF-TκB has been reported to play a role in de novo resistance of cancer cells to chemotherapeutic agents, which is a major cause for treatment failure in cancer chemotherapy. Previous studies have shown that 3,3'-diindolylmethane (DIM), a major in vivo acid-catalyzed condensation product of Indole-3-carbinol (I3C), is a potent inducer of apoptosis, inhibitor of tumor angiogenesis and inactivator of Akt/NF-κB signaling in breast cancer cells. We found that DIM can inhibit Akt and NF-κB in breast cancer cells, suggesting that DIM could sensitize the breast cancer cells to common chemotherapeutic agents. More recently, we found that DIM significantly sensitized the breast cancer cells to Taxotere and Adriamycin. However, little is known regarding the inactivation of Akt/NF-κB leading to chemosensitization of breast cancer cells to two of the most common chemotherapeutic agents such as Adriamycin and Taxotere. Based on our preliminary results, we hypothesize that DIM will inactivate Akt and NF-κB signaling, thereby sensitizing breast cancer cells to chemotherapeutic agents both in vitro as well as in vivo in an experimental model of breast cancer. The mechanisms for sensitizing the cells may involve down-regulation of the expression of NF-κB and its important regulators such as MEKK1, MEK, NIK and IKK genes. We believe that our strategies to sensitize breast cancer cells to the most common chemotherapeutic agents by DIM will be a novel breakthrough for devising optimal therapies for breast cancer.

15. SUBJECT TERMS
No subject terms provided

16. SECURITY CLASSIFICATION OF:			17. LIMITATION OF ABSTRACT	18. NUMBER OF PAGES	19a. NAME OF RESPONSIBLE PERSON USAMRMC
a. REPORT U	b. ABSTRACT U	c. THIS PAGE U	UU	31	19b. TELEPHONE NUMBER *(include area code)*

Standard Form 298 (Rev. 8-98)
Prescribed by ANSI Std. Z39.18

Table of Contents

Introduction

Constitutive activation of Akt or NF-κB has been reported to play a role in *de novo* resistance of cancer cells to chemotherapeutic agents, which is a major cause for treatment failure in cancer chemotherapy (1, 2). Previous studies have shown that 3,3'-diindolylmethane (DIM), a major *in vivo* acid-catalyzed condensation product of Indole-3-carbinol (I3C), is a potent inducer of apoptosis, inhibitor of tumor angiogenesis and inactivator of Akt/NF-κB signaling in breast cancer cells (3, 4). We found that DIM can inhibit Akt and NF-κB in breast cancer cells, suggesting that DIM could sensitize the breast cancer cells to common chemotherapeutic agents. More recently, we found that DIM significantly sensitized the breast cancer cells to Taxotere and Adriamycin. However, little is known regarding the inactivation of Akt/NF-κB leading to chemosensitization of breast cancer cells to two of the most common chemotherapeutic agents such as Adriamycin and Taxotere (5). Based on our preliminary results, we hypothesize that DIM will inactivate Akt and NF-κB signaling, thereby sensitizing breast cancer cells to chemotherapeutic agents both *in vitro* as well as *in vivo* in an experimental model of breast cancer. The mechanisms for sensitizing the cells may involve down-regulation of the expression of NF-κB and its important regulators such as MEKK1, MEK, NIK and IKK genes (5). We believe that our strategies to sensitize breast cancer cells to the most common chemotherapeutic agents by DIM will be a novel breakthrough for devising optimal therapies for breast cancer.

Body Report

The original statement of work in the proposal is listed below:

Task 1: To study the effect of 3, 3'-Diindolylmethane (DIM) on the inactivation of Akt/NF-κB signaling that may lead to the induction of apoptosis in breast cancer cells.

  a. We will investigate the NF-κB DNA-binding activity, cellular localization (by confocal microscopy), protein levels and the phosphorylation/de-phosphorylation of IκB in breast cancer cells by Western blot and phosphorylation studies (Months 1-3).

  b. We will also conduct apoptosis assays (ELISA, PARP, Caspase activation) and measure Akt (Western blot) and NF-κB (EMSA) under all conditions in order to correlate the degree of chemosensitization with inactivation of Akt/NF-κB (Months 1-3).

Task 2: To determine whether and how inactivation of Akt and NF-κB by DIM leads to chemosensitization of breast cancer cells to Adriamycin and Taxotere.

  a. We will conduct experiments by EMSA in cells transiently transfected with dominant negative IκB cDNA, NF-κB p65 cDNA, NF-κB-LUC, NF-κB mutant-LUC, cultured in the presence and absence of DIM, +/- Adriamycin and Taxotere to fully dissect the molecular pathways by which DIM elicits its effects on breast cancer cells (Months 3-6).

  b. We will investigate the molecular regulation of NF-κB through MEKK, IKK and NIK pathways by Western blot analysis and transfection studies in breast cancer cells transfected with or without constitutively activated Akt or dominant negative Akt in the presence and absence of DIM, +/- Adriamycin and Taxotere (Months 4-6).

  c. We will incubate breast cancer cells with DIM and subsequently treat with Adriamycin or Taxotere and the cells will be harvested for measuring cell growth inhibition by MTT assay and for measurement of apoptotic cell death by ELISA and CPP32 assays (Months 4-7).

Task 3: To investigate whether MDA-MB-231 breast cancer cells grown in SCID model require both expression of Akt and NF-κB, and to test whether DIM could sensitize the breast tumor to Adriamycin and Taxotere resulting in greater anti-tumor activity.

a. We will test whether or not DIM could sensitize the breast tumor to chemotherapeutic agents induced by MDA-MB-231 breast cancer cells grown in SCID model (Months 5-10).

b. We will also conduct apoptosis assays (ELISA, PARP, Caspase activation) and measure Akt (Western blot) and NF-κB (EMSA) under these conditions in order to correlate the degree of chemosensitization with inactivation of Akt/NF-κB (Months 5-11).

c. Frozen and paraffin sections of the s.c. grown tumors collected from the experiments will be used for molecular, histological and immunohistochemistry analysis for Akt, NF-κB and its upstream genes such as MEKK1, MEK, NIK and IKK as well as NF-κB downstream genes (Months 5-12).

d. We will summarize all the data, complete writing of all manuscripts, and submit the final report to DOD (Months 12).

Our progress was slow and we got an extension for one year with no cost. In fact we have been conducting a numerous experiments which are taking more time than anticipated previously. Hence, in order to demonstrate whether the chemo-enhancing effect of DIM is additive or synergistic, we need to do additional experiments and we will make progress on data analysis and manuscript writing during the extended year.

Although task 1, 2 and 3 are in progress, however we are now reporting the research accomplishment associated with task 1, 2 and 3 outlined in the statement of work:

MATERIAL AND METHODS

Cell culture and reagents

MDA-MB-231 human breast cancer cells (ATCC, Manassas, VA) were cultured in DMEM/F12 medium (Invitrogen) supplemented with 10% FBS and 1% penicillin/streptomycin in a 5% CO2 atmosphere at 37^0C. DIM (Bio Response, Boulder, Colorado) was dissolved in DMSO to make 20 mM stock solution and was added to the directly to the media at different concentration. Taxotere (Aventis Pharmaceuticals, Bridgewater, NJ) was dissolved in DMSO to make a 4µM stock solution.

Cell growth inhibition by 3-(4,5-dimethylthiazol-2-yl)-2,5-diphenyltetrazolium bromide assay

MDA-MB-231 cells were seeded in 96-well culture dishes. After 24 hours of incubation MDA-MB-231 were treated with 15, 30 or 45 µM DIM and then exposed to chemotherapeutic agents (0.5, 0.75 or 1.0 nM Taxotere) for 24, 48 or 72 hours. For single-agent treatment, MDA-MB-231 cells were treated with DIM (15, 30, or 45 µM), Taxotere (0.5, 0.75 or 1.0 nM) alone for 24 to 72 hours. After treatment, cancer cells were incubated with 3-(4,5-dimethylthiazol-2-yl)-2,5 diphenyltetrazolium bromide (MTT; 0.5 mg/mL, Sigma) at 37^0C for 2 hours and then with isopropyl alcohol at room temperature for 1 hour. The spectrophotometric absorbance of the samples was determined by ULTRA Multifunctional Microplate Reader (TECAN, Durham,NC) at 595 nm.

Histone/DNA ELISA for detecting apoptosis

Cell Apoptosis ELISA Detection Kit (Roche, Palo Alto, CA) was used to detect apoptosis according to the protocol of the manufacturer. Briefly, MDA-MB-231 cells were treated with DIM and/or chemotherapeutic agents (Taxotere) as described above. After treatment, the cytoplasmic histone/DNA fragments from cancer cells with different treatments were extracted and bound to immobilized anti-histone antibody. Subsequently, the peroxidase-conjugated anti-DNA antibody was used for the detection of immobilized histone/DNA fragments. After addition of substrate for

peroxidase, the spectrophotometric absorbance of the samples was determined by ULTRA Multifunctional Microplate Reader (TECAN) at 405 nm.

Nuclear factor KB DNA-binding activity measurement

MDAMB- 231 cells were plated at a density of $1x10^5$ cells in 100 mm dishes and incubated. After 24 hours, the cells were treated with combination of DIM and chemotherapeutic agents as described above. For single-agent treatment, cancer cells were treated with DIM (30 or 45 µM), 1 nM Taxotere alone for 2 hours. Following treatments, nuclear protein in the cells was extracted as described previously (3, 6-8). For electrophoretic mobility shift assay (EMSA), 10 Ag of nuclear protein were assembled with 5x Gel Shift Binding buffer (20% glycerol, 5 mmol/L MgCl2, 2.5 mmol/L EDTA, 2.5 mmol/L DTT, 250 mmol/L NaCl, 50 mmol/L Tris-HCl), 0.25 mg/mL poly(dI)-poly(dC), and IRDye 700-labeled NF-nB oligonucleotide (LI-COR, Lincoln, NE). After incubation at room temperature for 30 minutes, the samples were loaded on a pre-run 8% polyacrylamide gel and electrophoresis was continued at 30 mA for 90 minutes. The signal was then detected and quantified with Odyssey infrared imaging system (LI-COR).
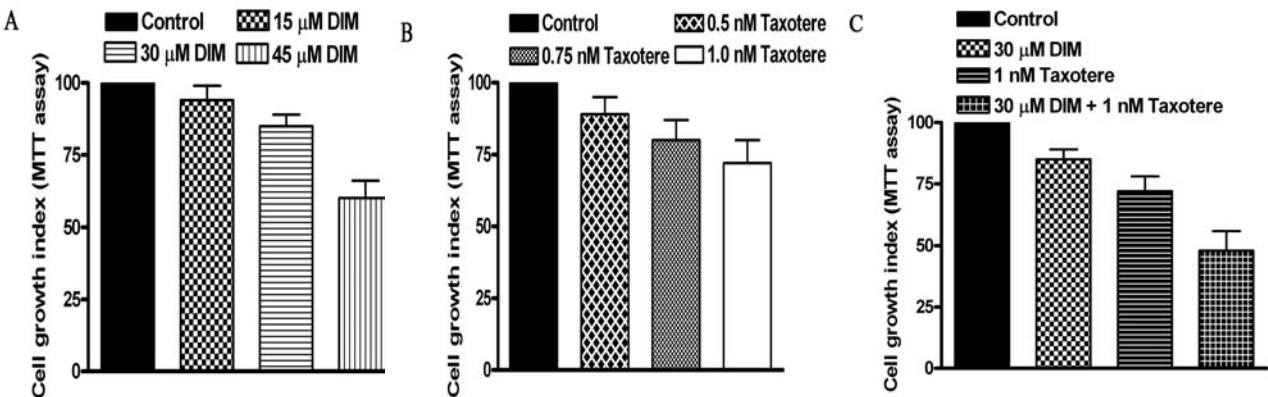
RESULTS:

A. DIM potentiated cancer cell growth inhibition caused by chemotherapeutic agents

MDA-MB-231 breast cancer cells were treated with DIM, Taxotere, or DIM in combination with lower doses of Taxotere. The cell viability was determined by MTT assay, and the effect of DIM or Taxotere on the growth of different cancer cells is shown in Fig. 1 A and B. We found that treatment of cells with DIM or Taxotere alone for 72 hours commonly caused ~ 30 % growth inhibition in cancer cells using the doses tested. However, DIM in combination with lower doses of Taxotere resulted in ~ 50% growth inhibition in these cancer cells suggesting the synergistic effect of each combination treatment (Fig 1C). These results showed that combination of DIM with lower
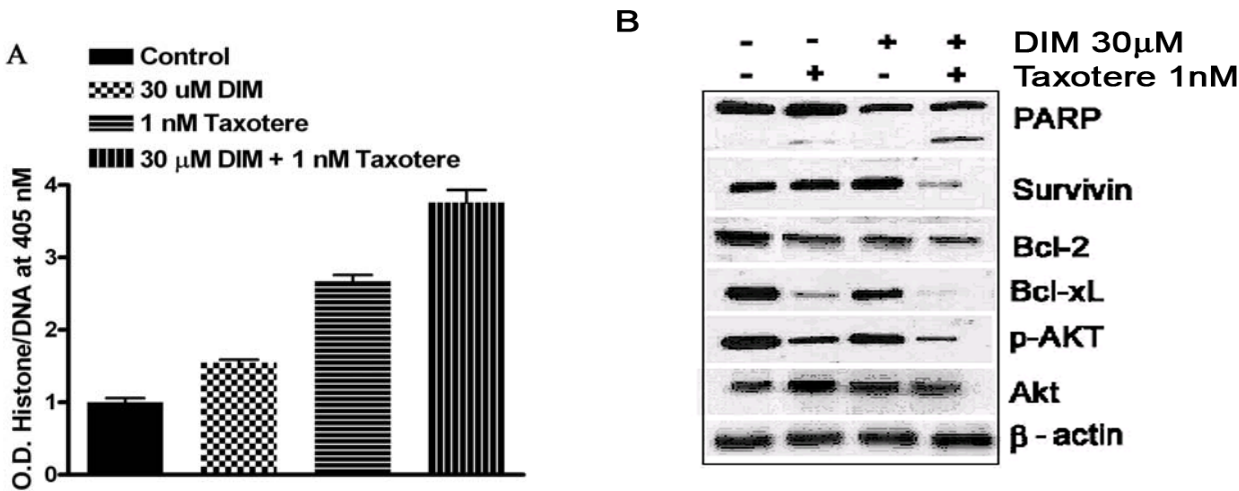
doses of Taxotere elicited significantly greater inhibition of cancer cell growth compared with either agent alone.

Figure 1:

B. DIM sensitized cancer cells to apoptosis induced by chemotherapeutic agents
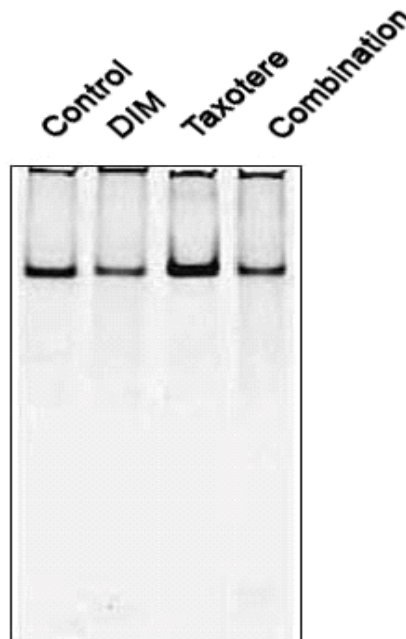
Figure 2:

By apoptotic cell death ELISA we observed similar results showing that DIM or Taxotere induced apoptosis in breast cancer cells tested (Fig. 2A). Moreover, we found that 30 µM DIM combined with lower doses of Taxotere induced more apoptosis in the cancer cells compared with

single-agent treatment (Fig. 2A). We also observed that DIM and Taxotere combination treatment produced more PARP cleavages compared with monotreatment (Fig. 2B), suggesting more apoptosis induced by the combination treatment *in vitro*. By Western blot analysis, we found that DIM alone or in combination with chemotherapeutic agents down-regulated the expression of survivin, Bcl-2, and Bcl-X$_L$, p-Akt in breast cancer cells (Fig. 2 B). These results are consistent with cell growth inhibition observed by MTT assay, suggesting that greater cell growth inhibition by combination treatment may be mediated through the induction of more apoptosis in cancer cells.

C. DIM abrogated activation of nuclear factor κB activity stimulated by Taxotere *in vitro*.

Figure 3:

We next looked into molecular basis for chemo-resistance by performing EMSA in MDA-MB-231 breast cancer cell using Taxotere and DIM. Nuclear proteins from cultured cancer cells treated with DIM and Taxotere were subjected to analysis for NF-κB DNA-binding activity as measured by EMSA. Our findings clearly showed that Taxotere induces NF-κB which can be down-regulated by combination treatment (Fig 3). These results provide mechanistic support in favor of our claim that the apoptosis-inducing effect of Taxotere is enhanced by DIM and it is partly mediated through the NF-κB pathway.

KEY RESEARCH ACCOMPLISHMENT

1. Our results showed that combination of DIM with lower doses of Taxotere elicited significantly greater inhibition of cancer cell growth compared with either agent alone.

2. Collectively our present results clearly suggest that inhibition of NF-κB signaling by DIM leads to chemosensitization of breast cancer cells to Taxotere which may contribute to increased growth inhibition and apoptosis in breast cancer cells.

REPORTABLE OUTCOMES

1. **Rahman KM,** Li Y, Wang Z, Sarkar SH, Sarkar FH (2006). Gene expression profiling revealed survivin as a target of DIM-induced cell growth inhibition and apoptosis in breast cancer cells. Cancer Research, 66(9), 4952-60.

2. **Rahman, KM,** Fazlul H. Sarkar, Sanjeev Banerjee, Zhiwei Wang, Dezhong Liao, Xin Hong and Nurul H. Sarkar (2006). Therapeutic intervention of experimental breast cancer bone metastasis by Indole-3-carbinol in SCID-hu mouse model. Mol Cancer Ther 2006;5(11):2747–56.

CONCLUSIONS

In conclusion, out present results clearly show that DIM inactivates NF-κB and, in turn, sensitizes cancer cell to growth inhibition and apoptosis induced by chemotherapeutic agents such as Taxotere. However, further in-depth studies including clinical trials are needed to fully evaluate the value of DIM in combination with chemotherapeutic agents such as Taxotere for the treatment of human cancers.

REFERENCES

1.   Haefiner, B., Nf-kappaB:arresting a major culprit in cancer. Drug Discov. 7:653-663, 2002.

2. Clark, A.S., West, K., Streicher, S., et al., Constitutive and inducible Akt activity promotes resistance to chemotherapy, trastuzumab, or tamoxifen in breast cancer cells. Mol Cancer Ther 1:707-717, 2002.

3. Rahman, K.W. and Sarkar, F.H., Inhibition of nuclear translocation of nuclear factor-{kappa}B contributes to 3,3'-diindolylmethane-induced apoptosis in breast cancer cells. Cancer Res 65:364-371, 2005.

4. Chang, X., Tou, J.C., Hong, C., et al., 3,3'-diindolylmethane inhibits angiogenesis and the growth of transplantable human breast carcinoma in athymic mice. Carcinogenesis, 2005.

5. Fuino, L., Bali, P., Wittmann, S., et al., Histone deacetylase inhibitor LAQ824 down-regulates Her-2 and sensitizes human breast cancer cells to trastuzumab, taxotere, gemcitabine, and epothilone B. Mol Cancer Ther 2:971-984, 2003.

6. Rahman, K.M., Li, Y., Sarkar, F.H., Inactivation of akt and NF-kappaB play important roles during indole-3-carbinol-induced apoptosis in breast cancer cells. Nutr Cancer 48:84-94, 2004.

7. Rahman, K.M., Sarkar, F.H., Banerjee, S., et al., Therapeutic intervention of experiemntal breast cancer metastasis by Indole-3-carbinol in SCID-hu mouse model. Mol Cancer Ther 2006;5(11):2747–56.

8. Rahman, K.W., Li, Y., Wang, Z., et al., Gene expression profiling revealed survivin as a target of 3,3'-diindolylmethane-induced cell growth inhibition and apoptosis in breast cancer cells. Cancer Res 66:4952-4960, 2006.

Gene Expression Profiling Revealed Survivin as a Target of 3,3′-Diindolylmethane-Induced Cell Growth Inhibition and Apoptosis in Breast Cancer Cells

KM Wahidur Rahman, Yiwei Li, Zhiwei Wang, Sarah H. Sarkar, and Fazlul H. Sarkar

Department of Pathology, Karmanos Cancer Institute, Wayne State University School of Medicine, Detroit, Michigan

Abstract

The phytochemical indole-3-carbinol (I3C), found in cruciferous vegetables, and its major acid-catalyzed reaction product 3,3′-diindolylmethane (DIM) showed anticancer activity mediated by its pleiotropic effects on cell cycle progression, apoptosis, carcinogen bioactivation, and DNA repair. To further elucidate the molecular mechanism(s) by which 3,3′-diindolylmethane exerts its effects on breast cancer cells, we have used microarray gene expression profiling analysis. We found a total of 1,238 genes altered in 3,3′-diindolyl-methane-treated cells, among which 550 genes were down-regulated and 688 genes were up-regulated. Clustering analysis showed significant alterations in some genes that are critically involved in the regulation of cell growth, cell cycle, apoptosis, and signal transduction, including down-regulation of survivin. Previous studies have shown that antiapoptotic protein survivin is overexpressed in many human cancers, including breast cancer. However, very little or no information is available regarding the consequence of down-regulation of survivin for cancer therapy. We, therefore, hypothesized that down-regulation of survivin as observed by 3,3′-diindolylmethane could be an important approach for the treatment of breast cancer. We have tested our hypothesis using multiple molecular approaches and found that 3,3′-diindolylmethane inhibited cell growth and induced apoptosis in MDA-MB-231 breast cancer cells by down-regulating survivin, Bcl-2, and cdc25A expression and also caused up-regulation of $p21^{WAF1}$ expression, which could be responsible for cell cycle arrest. Down-regulation of survivin by small interfering RNA before 3,3′-diindolylmethane treatment resulted in enhanced cell growth inhibition and apoptosis, whereas overexpression of survivin by cDNA transfection abrogated 3,3′-diindolylmethane-induced cell growth inhibition and apoptosis. These results suggest that targeting survivin by 3,3′-diindolylmethane could be a new and novel approach for the prevention and/or treatment of breast cancer. (Cancer Res 2006; 66(9): 4952-60)

Introduction

Breast cancer is the second leading cause of cancer-related deaths in women in the United States (1), suggesting that early diagnosis and prevention of this disease is urgently needed. Currently, breast cancer is treated with surgery, chemotherapy, and radiation therapy or combined modalities with remarkable success. In addition, patients with breast cancer or preneoplastic lesions are also treated with hormonal therapy either for treatment or prevention purposes. Although these treatment modalities are successful, a significant number of patients either do not respond to therapy, or the tumor may recur during therapy and develop metastasis, for which there is limited curative therapy. This inadequate outcome strongly suggests that the evaluation of novel targeted therapeutic agents is urgently needed to improve the treatment outcome of patients diagnosed with this disease.

It has been well known that many genes play important roles in the control of cell growth, differentiation, apoptosis, inflammation, stress response, and many other physiologic processes (2–10). Among those genes, *survivin*, a member of the inhibitor of apoptosis protein (IAP) family, plays important roles in tumorigenesis, progression of breast carcinoma, cell invasion, metastasis, and resistance to chemotherapy (10–15). Several studies have suggested that the antiapoptotic protein survivin is overexpressed in many human cancers, including breast cancer (9, 10). It has also been shown that expression of survivin is associated with cancer cell viability and drug resistance (16). Previous studies in determining the association of survivin with prognosis in breast cancer patients has been controversial (17); thus, the clinical importance of survivin expression remains unclear in patients with breast cancer. We believe that the down-regulation of survivin in breast cancer cells could be a novel therapeutic approach for achieving optimal results in patients with chemoresistant breast cancer. However, very little or no information is currently available regarding the consequence of down-regulation of survivin in cell fate and whether this down-regulation could offer potential therapeutic benefits in breast cancer patients.

Studies from our laboratory and others have shown that 3,3′-diindolylmethane, a major *in vivo* acid-catalyzed condensation product of indole-3-carbinol (I3C), is a potent inhibitor of cell growth and inducer of apoptotic cell death (4, 18–22). However, the comprehensive molecular mechanism(s) by which I3C/3,3′-diindolylmethane inhibits cell growth and apoptosis is still unknown. However, the 3,3′-diindolylmethane's pleiotropic effects on breast cancer cells could be due to alterations in gene expression profiles that are important for cell growth and induction of apoptosis. Thus, understanding the molecular biological properties of 3,3′-diindolylmethane may lead to the clinical development of mechanism-based chemopreventive and/or therapeutic strategies for breast cancer. Microarray gene expression profiling allows examination of the expression of a large number of genes and, in turn, provides an opportunity for determining the effects of anticancer agents on cancer cells. The alterations of gene expression profiles by several anticancer agents have been reported (23, 24). In this study, we used the high-throughput gene chip, which contains 22,215 known genes to better understand the

precise molecular mechanism(s) by which 3,3′-diindolylmethane exerts its effects on breast cancer cells. We found a total of 1,238 genes altered by 3,3′-diindolylmethane treatment, among which 550 genes were down-regulated and 668 genes were up-regulated, many of which are associated with regulation of cell growth, cell cycle, apoptosis, and intracellular signaling. We also found a significant down-regulation of survivin expression. Based on our results, we further tested and found that 3,3′-diindolylmethane-induced down-regulation of survivin is, in part, mechanistically associated with 3,3′-diindolylmethane-induced cell growth inhibition and apoptosis.

Materials and Methods

Cell culture and growth inhibition. For the present study, we have used human breast epithelial cells MDA-MB-231, which is tumorigenic [American Type Culture Collection (ATCC), Manassas, VA]. It has aggressive invasion capacity and can also grow very well in an animal model (ATCC). MDA-MB-231 was grown in DMEM/F12 (Invitrogen, Carlsbad, CA) supplemented with 10% fetal bovine serum and 1% penicillin and streptomycin in a 5% CO_2 atmosphere at 37°C. 3,3′-Diindolylmethane (LKT Laboratories, St. Paul, MN) was dissolved in DMSO to make 20 mmol/L stock solution and was added directly to the media at different concentrations. Concentration between 30 and 60 μmol/L 3,3′-diindolylmethane seems adequate for this study primarily because results of several studies have indicated that 3,3′-diindolylmethane exhibits promising cancer protective activities, especially against mammary neoplasia (8, 25–28). Moreover, based on these previous studies, including our own study, we have chosen different concentrations of 3,3′-diindolylmethane for this study, which is relevant and achievable *in vivo*. Survivin small interfering RNA (siRNA) and siRNA control were obtained from Santa Cruz Biotechnology (Santa Cruz, CA). LipofectAMINE 2000 was purchased from Invitrogen. Protease inhibitor cocktail, 3-(4,5-dimethylthiazol-2-yl)-2,5-diphenyltetrazolium bromide (MTT), and all other chemicals were obtained from Sigma (St. Louis, MO).

Cell growth inhibition studies by MTT assay. For growth inhibition, MDA-MB-231 cells (2×10^3) were seeded in a 96-well culture plate and subsequently treated with 10, 20, 30, 40, and 60 μmol/L 3,3′-diindolylmethane for 24, 48, and 72 hours, whereas control cells received 0.01% DMSO in culture medium. After treatment, the cells were incubated with MTT reagent (0.5 mg/mL; Sigma) at 37°C for 2 hours and then with isopropanol at room temperature for 1 hour. Spectrophotometric absorbance of the samples was determined by an Ultra Multifunctional Microplate Reader (Tecan, Durham, NC). Results were plotted as means ±SD of three separate experiments having six determinations per experiment for each experimental condition.

Histone/DNA ELISA for detecting apoptosis. The cell apoptosis ELISA detection kit (Roche, Palo Alto, CA) was used to detect apoptosis in breast cancer cells treated with 3,3′-diindolylmethane according to manufacturer's protocol. Briefly, the cytoplasmic histone/DNA fragments from MDA-MB-231 breast cancer cells treated with 40 and 60 μmol/L 3,3′-diindolylmethane or DMSO (vehicle control) for 24, 48, or 72 hours were extracted and bound to immobilized anti-histone antibody. Subsequently, the peroxidase-conjugated anti-DNA antibody was used for the detection of immobilized histone/DNA fragments. After addition of substrate for peroxidase, the spectrophotometric absorbance of the samples was determined by using Ultra Multifunctional Microplate Reader at 405 nm.

Plasmid and transfection. The survivin cDNA plasmid encoding survivin were obtained from Science Reagents (Ipswich, MA). MDA-MB-231 cells were transfected with survivin siRNA and siRNA control, respectively, using LipofectAMINE 2000. MDA-MB-231 cells were transiently transfected with human survivin cDNA. The transfected cells were treated with 40 and 60 μmol/L 3,3′-diindolylmethane for 24, 48, and 72 hours or kept as control. The cell growth and apoptotic cell death of transfected cells with and without treatments were measured using MTT assay and cell apoptosis ELISA Detection kit (Roche), respectively.

cDNA microarray analysis. MDA-MB-231 cells were treated with 40 μmol/L 3,3′-diindolylmethane for 6, 24, and 48 hours. 3,3′-Diindolylmethane is the *in vivo* dimeric product of I3C. The doses of 3,3′-diindolylmethane chosen for the microarray experiment were close to IC_{50}. However, the biological relevance of these doses in relation to prevention or therapy has not been fully evaluated. The rationale for choosing these time points was to capture the expression profiles of early-response genes, genes that may be involved in the onset of growth inhibition and apoptotic processes, and, finally, genes that may be involved during active growth inhibition and apoptosis. Total RNA from each sample was isolated by Trizol (Invitrogen) and purified using the RNeasy Mini kit and RNase-free DNase Set (Qiagen, Valencia, CA) according to the manufacturer's protocols. cDNA for each sample was synthesized using a Superscript cDNA Synthesis kit (Invitrogen) and a T7-(dT)24 primer instead of the oligo-(dT) provided in the kit. Then, the biotin-labeled cRNA was transcribed *in vitro* from cDNA using a BioArray HighYield RNA Transcript Labeling kit (ENZO Biochem, New York, NY) and purified using the RNeasy Mini kit. The purified cRNA was fragmented by incubation in fragmentation buffer [200 mmol/L Tris-acetate (pH 8.1), 500 mmol/L potassium acetate, 150 mmol/L magnesium acetate] at 95°C for 35 minutes and chilled on ice. The fragmented labeled cRNA was applied to the Human Genome U133A Array (Affymetrix, Santa Clara, CA), which contains 22,215 human gene sequence, and hybridized to the probes in the array. After washing and staining, the arrays were scanned using a HP GeneArray Scanner (Hewlett-Packard, Palo Alto, CA). Two independent experiments were done to verify the reproducibility of our results.

Microarray data normalization and analysis. The gene expression levels of samples were normalized and analyzed using Microarray Suite, MicroDB and Data Mining Tool software (Affymetrix). The signal value of the experimental array was multiplied by a normalization factor to make its mean intensity equivalent to the mean intensity of the control array using Microarray Suite software according to manufacturer's protocol. The absolute call (present, marginal, and absent) and average difference of 22,215 gene expressions in a sample and the absolute call difference, fold change, and average difference of gene expressions between two or several samples were identified using the abovementioned software. Statistical analysis of the difference in the mean expression of genes showing a >2-fold change was done repeatedly between treated and untreated samples using *t* tests. Average-linkage hierarchical clustering of the data was applied using the Cluster method (29), and the results were displayed with TreeView (29). The genes showing altered expression were also categorized based on their location and cellular component and reported or suggested biochemical, biological, and molecular functions using Onto-Express (30). Genes that were not annotated or not easily classified were excluded from the functional clustering analysis.

Real-time reverse transcription-PCR analysis for gene expression. To verify the alterations of gene expression at the mRNA level, which appeared on the microarray, we chose 15 representative genes (Table 2) with varying expression profiles for real-time reverse transcription-PCR (RT-PCR) analysis. Two micrograms of total RNA from each sample were subjected to reverse transcription using the Superscript first-strand cDNA synthesis kit (Invitrogen) according to the manufacturer's protocol. Real-time PCR reactions were then carried out in a total of 25 μL of reaction mixture (2 μL of cDNA, 12.5 μL of 2× SYBR Green PCR Master Mix, 1.5 μL of each 5 μmol/L forward and reverse primers, and 7.5 μL of H_2O) in an ABI Prism 7700 Sequence Detection System (Applied Biosystems, Foster City, CA). The PCR program was initiated for 10 minutes at 95°C before 40 thermal cycles, each of 15 seconds at 95°C, and 1 minute at 60°C. Data was analyzed according to the comparative C_t method and was normalized by actin expression in each sample. Melting curves for each PCR reaction were generated to ensure the purity of the amplification product.

Western blot analysis. To verify whether the alterations of genes at the level of transcription ultimately result in the alterations at the level of translation, we conducted Western blot analysis for selected genes with varying expression profiles. The MDA-MB-231 cells were treated with 40 and 60 μmol/L 3,3′-diindolylmethane for 6, 12, and 48 hours. After treatment, the cells were lysed, and protein concentration was measured
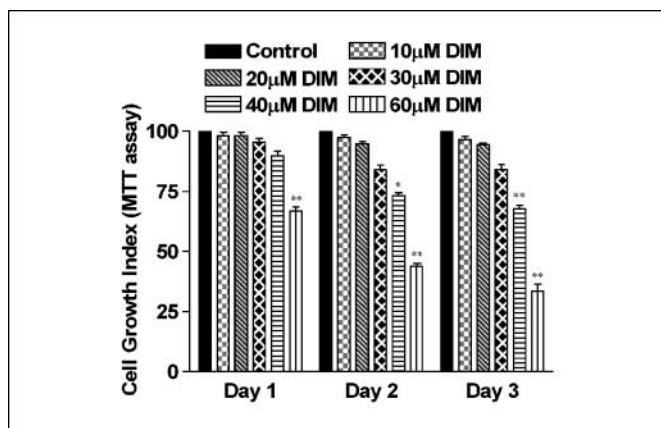
Figure 1. Effects of 3,3′-diindolylmethane (*DIM*) on the growth of MDA-MB-231 cells. MDA-MB-231 breast cancer cells were treated with 3,3′-diindolylmethane, showing inhibition of cell proliferation in a dose-dependent and time-dependent manner. The proliferation of MDA-MB-231 cells was significantly inhibited by 40 μmol/L 3,3′-diindolylmethane treatment for 48 and 72 hours (30% and 40%, respectively) compared with 60 μmol/L 3,3′-diindolylmethane treatment for 24, 48, and 72 hours (40%, 60%, and 70%, respectively). *, $P < 0.05$; **, $P < 0.01$.

using bicinchoninic acid protein assay (Pierce, Rockford, IL). The proteins were subjected to 10%, 12%, or 14% SDS-PAGE and electrophoretically transferred to nitrocellulose membrane. The membranes were incubated with anti-p21[WAF1] (1:500; Upstate, Lake Placid, NY), anti-survivin (1:200; R&D Systems, Minneapolis, MN), anti-cell division cycle cdc25A (1:200; Santa Cruz Biotechnology), anti-Bcl-2 (1:250; Calbiochem, San Diego, CA), and anti-β-actin (1:10,000; Sigma) primary antibodies and subsequently incubated with the secondary antibodies conjugated with peroxidase. All secondary antibodies were obtained from Pierce. The signal was then detected using chemiluminescence detection system (Pierce).

Statistical analysis. The statistical significance was determined using Student's *t* test, and $P < 0.05$ was considered significant.

Results

Cell growth inhibition by 3,3′-diindolylmethane treatment. MTT assay showed that the treatment of MDA-MB-231 breast cancer cells with 3,3′-diindolylmethane resulted in a dose- and time-dependent inhibition of cell proliferation (Fig. 1), showing the inhibitory effect of 3,3′-diindolylmethane on MDA-MB-231 cell growth. The proliferation of MDA-MB-231 cells was significantly inhibited by 40 μmol/L 3,3′-diindolylmethane treatment for 48 and 72 hours (30% and 40%, respectively) compared with 60 μmol/L 3,3′-diindolylmethane treatment for 24, 48, and 72 hours (40%, 60%, and 70%, respectively). These results are consistent with our previously published results (8). Inhibition of cell proliferation observed by MTT could be due to altered regulation of several gene expressions by 3,3′-diindolylmethane treatment. Hence, we further investigated the gene expression profile of MDA-MB-231 breast cancer cells treated with 3,3′-diindolylmethane.

Regulation of the mRNA expression by 3,3′-diindolylmethane treatment. The gene expression profile of MDA-MB-231 breast cancer cells treated with 3,3′-diindolylmethane was assessed using cDNA microarray. We found a total of 1,238 genes that showed a >1.5-fold change after 48 hours of 3,3′-diindolylmethane treatment. Among these genes, 550 genes were down-regulated, and 688 genes were up-regulated in 3,3′-diindolylmethane-treated MDA-MB-231 breast cancer cells. The altered expressions of most
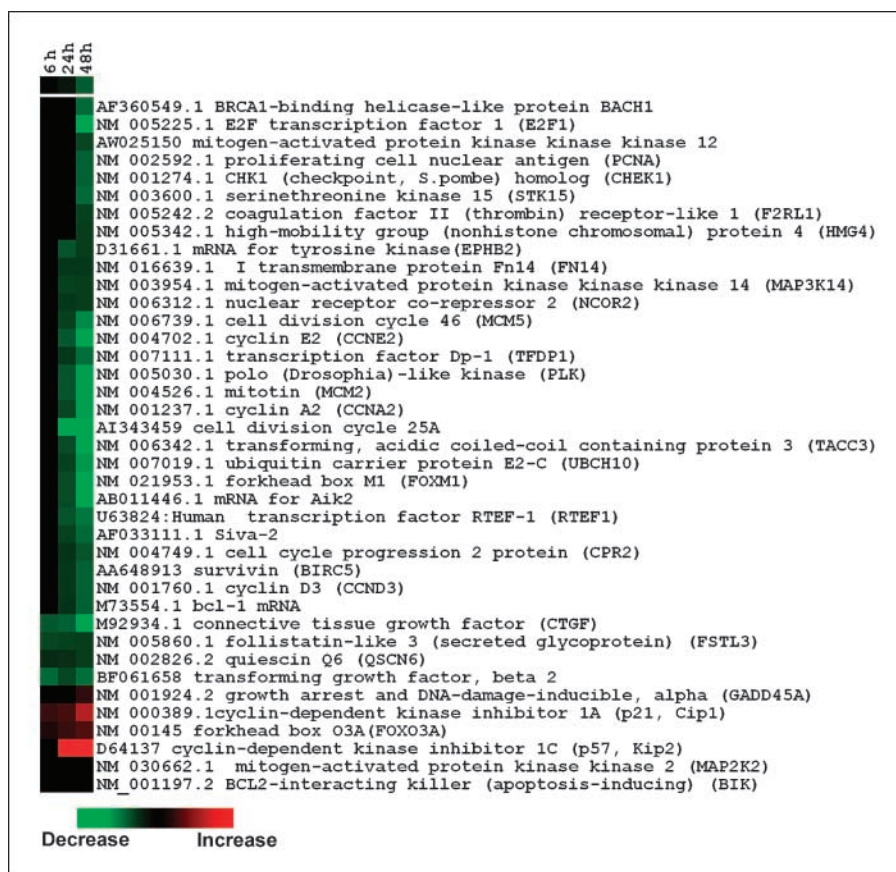

Figure 2. Cluster analysis of genes showing alterations in mRNA expression after 3,3′-diindolylmethane treatment. The alterations of specific and selected genes are shown.

Table 1. Fold changes of specific genes in MDA-MB-231 cells treated with 3,3′-diindolylmethane

Genes	MDA-MB-231		
	6 h	24 h	48 h
Cell cycle, apoptosis, and cell proliferation			
NM_004702.1, cyclin E2 (*CCNE2*)	NC	−2.2*	−4.2
AI343459, cdc25A	NC	−6.9	−13.9
NM_001760.1, cyclin D3 (*CCND3*)	NC	−1.5	−2.4
NM_001197.2, BCL2-interacting killer (apoptosis-inducing; BIK)	NC	NC	NC
NM_004749.1, cell cycle progression 2 protein (*CPR2*)	NC	−1.4	−2.1
NM_006739.1, cdc46 (*MCM5*)	NC	−1.7	−3.4
NM_002592.1, proliferating cell nuclear antigen (*PCNA*)	NC	NC	−2.5
NM_004526.1, mitotin (*MCM2*)	NC	−2.1	−4.0
NM_001237.1, cyclin A2 (*CCNA2*)	NC	−1.8	−4.0
AA648913, survivin (*BIRC5*)	NC	−1.5	−2.4
AF033111.1, Siva-2	NC	−1.7	−2.6
NM_005860.1, follistatin-like 3 (secreted glycoprotein; *FSTL3*)	−1.8	−1.7	−1.6
AB011446.1, mRNA for Aik2	NC	−2.0	−4.9
M73554.1, bcl-1 mRNA	NC	−1.4	−2.4
NM_001924.2, growth arrest and DNA damage–inducible, alpha (*GADD45A*)	NC	NC	1.4
NM_005030.1, polo (*Drosophila*)-like kinase (*PLK*)	NC	−2.1	−4.0
D64137, CDK inhibitor 1C ($p57^{Kip2}$)	NC	22.6 [†]	6.9 [†]
NM_000389.1, CDK inhibitor 1A ($p21^{Cip1}$)	1.51	1.7 [†]	4.0 [†]
BF061658, transforming growth factor-β2	−2.6	−1.8	−2.8
NM_00145, FOXO3A	1	1.6	2
Kinase, cell signaling, and cell structure			
NM_003954.1, mitogen-activated protein kinase kinase kinase 14 (*MAP3K14*)	NC	−1.7	−1.6
NM_030662.1, mitogen-activated protein kinase kinase 2 (*MAP2K2*)	NC	NC	NC
AW025150, mitogen-activated protein kinase kinase kinase 12	NC	NC	−1.8
D31661.1, mRNA for tyrosine kinase (*EPHB2*)	NC	−2.1	−1.6
NM_007019.1, ubiquitin carrier protein E2-C (*UBCH10*)	NC	−1.7	−3.7
Transcription and translation			
NM_021953.1, forkhead box M1 (*FOXM1*)	NC	−2.0	−4.5
NM_005225.1, E2F transcription factor 1 (*E2F1*)	NC	NC	−4.2
AF360549.1, BRCA1-binding helicase-like protein *BACH1*	NC	NC	−2.6
NM_005342.1, high-mobility group (nonhistone chromosomal) protein 4 (*HMG4*)	1.1	NC	−1.6
U63824, human transcription factor RTEF-1 (*RTEF1*)	NC	−2.1	−3.0
NM_006312.1, nuclear receptor corepressor 2 (*NCOR2*)	NC	−1.5	−1.6
NM_007111.1, transcription factor Dp-1 (*TFDP1*)	NC	−1.5	−2.8
Angiogenesis, metastasis, and invasion			
M92934.1, connective tissue growth factor (*CTGF*)	−2.2	−2.4	−6.9
NM_006342.1, transforming, acidic coiled-coil containing protein 3 (*TACC3*)	NC	−2.0	−4.2
NM_016639.1, I transmembrane protein Fn14 (*FN14*)	NC	−1.6	−1.5
NM_002826.2, quiescin Q6 (*QSCN6*)	−1.2	−1.3	−1.6
NM_005242.2, coagulation factor II (thrombin) receptor-like 1 (*F2RL1*)	NC	NC	−1.7
NM_003600.1, serine-threonine kinase 15 (*STK15*)	NC	NC	−2.6
NM_001274.1, CHK1 (checkpoint, *Schizosaccharomyces pombe*) homologue (*CHEK1*)	NC	NC	−2.4

Abbreviation: NC, no change.
*Negative value, decrease.
†Positive value, increase.

genes occurred after only 6 hours of 3,3′-diindolylmethane treatment and were more evident with longer treatment (Fig. 2). After clustering based analysis according to their biological functions, we found down-regulation and up-regulation of several genes, which are related to apoptosis, angiogenesis, tumor cell invasion, and metastasis (Fig. 2; Table 1).

Target confirmation by real-time RT-PCR. To confirm these alterations in gene expression, we conducted RT-PCR analysis of selected genes (Table 2). The results of RT-PCR analysis for these selected genes (*BACH1, BIRC5, CCNE2, cdc25A, F2F1, FOXM1, MCM5, $p21^{Cip1}$, $p57^{Kip2}$, PCNA, TACC3*, and *UBCH10*) were in direct agreement with the microarray data (Fig. 3*A*; Table 1). The same alternations at the mRNA levels were observed by RT-PCR analysis after 3,3′-diindolylmethane treatment, although the fold change in the expression level was not exactly similar between these two different analytic methods (Fig. 3*A*; Table 1). To further verify the regulation of gene expression at the protein level by 3,3′-diindolyl-methane treatment, we narrowed down few genes from the

RT-PCR analysis and conducted Western blot analysis only for selected few genes, which are the main focus of this study and for those genes that are critically important for the inhibition of cell growth and induction of apoptosis. Western blot analysis showed that the protein levels of BIRC5 (survivin), Bcl-2, and cdc25A were down-regulated, and p21^{WAF1} was up-regulated after 3,3′-diindolylmethane treatment (Fig. 3B). These results suggest that 3,3′-diindolylmethane regulated the transcription of the genes involved in apoptosis and cell cycle arrest, angiogenesis, tumor cell invasion, and metastasis, and these results are consistent with our previously published data in prostate cancer cells (3).

Regulation of genes involved in cell cycle and apoptotic process. After clustering based on biological function using OntoExpress and GenMAPP computerized analysis, we found that in MDA-MB-231 breast cancer cells, 3,3′-diindolylmethane down-regulated the expression of some genes that are critically involved in the regulation of cell proliferation and cell cycle (Table 1; Figs. 2 and 4). In contrast, 3,3′-diindolylmethane up-regulated the expression of some genes that are related to induction of apoptosis and cell cycle arrest (Table 1; Figs. 2 and 4). Western blot analysis showed that the protein levels of p21^{WAF1} in MDA-MB-231 cells treated for 48 hours with 3,3′-diindolylmethane were up-regulated, whereas survivin, Bcl-2, and cdc25A were down-regulated (Fig. 3B). These results are novel and have not been previously shown. These results are also in direct agreement with the microarray and RT-PCR data. In addition to the effects of 3,3′-diindolylmethane on cell cycle and apoptosis, 3,3′-diindolylmethane also showed the

regulation of genes related to signal transduction, transcription factor, oncogenesis, and tumor suppression (Table 1; Fig. 2). However, among these genes, *survivin* may have different roles in apoptosis in breast cancer, and because the clinical importance of survivin expression remains unclear in patients with breast cancer, we further investigated the mechanistic role of survivin during 3,3′-diindolylmethane-induced cell growth inhibition and apoptosis.

Down-regulation of survivin expression by siRNA promotes 3,3′-diindolylmethane-induced cell growth inhibition and apoptosis. We used Western blot analysis to detect the protein level of survivin. Intracellular survivin was down-regulated in survivin siRNA–transfected MDA-MB-231 cells compared with siRNA control–transfected cells (Fig. 5). Down-regulation of survivin expression significantly attenuated cell growth inhibition induced by 3,3′-diindolylmethane (Fig. 6A). We found that treatment of cells with 3,3′-diindolylmethane or survivin siRNA alone for 72 hours generally caused 60% to 70% of growth inhibition in MDA-MB-231 cells compared with control. However, 3,3′-diindolylmethane plus survivin siRNA resulted in ∼90% growth inhibition compared with control. Survivin siRNA–transfected MDA-MB-231 cells were significantly more sensitive to spontaneous and 3,3′-diindolylmethane-induced apoptosis (Fig. 6B). These results suggest that 3,3′-diindolylmethane plus survivin siRNA promotes cell growth inhibition and apoptosis to a greater degree compared with either agent alone.

Overexpression of survivin by cDNA transfection reduced 3,3′-diindolylmethane-induced cell growth inhibition and apoptosis. Overexpression of survivin by cDNA transfection rescued 3,3′-diindolylmethane-induced cell growth inhibition and abrogated 3,3′-diindolylmethane-induced apoptosis to a certain degree (Fig. 6C and D). We found that treatment of cells with survivin cDNA for 72 hours promotes ∼90% of cell growth in MDA-MB-231 cells compared with control. However, 3,3′-diindolylmethane plus survivin cDNA resulted in ∼35% growth inhibition compared with control (Fig. 6C). These results provide evidence for a potential role of survivin during 3,3′-diindolylmethane-induced cell growth inhibition and apoptosis in MDA-MD-231 cells.

Discussion

In the present study, we showed that 3,3′-diindolylmethane elicits a significant effect on growth inhibition and induction of apoptotic processes in MDA-MB-231 breast cancer cells mediated by alterations in the gene expression of cell cycle and apoptosis regulatory genes as shown by microarray analysis. Among these genes, we found down-regulation of several genes, such as *BACH1*, *BIRC5* (*survivin*), *CCNE2*, *CDC25A*, *Bcl-2*, *E2F1*, *FOXM1*, *MCM5*, *PCNA*, *TACC3*, *UBCH10*, *Aik2*, and *CTGF*, and up-regulation of several genes, such as *p21^{Cip1}*, *p57^{Kip2}*, and *FOXO3A*, in 3,3′-diindolylmethane-treated MDA-MB-231 cells that are related to the inhibition of cell growth and induction of apoptosis. To further elucidate the mechanisms of increased apoptosis induced by 3,3′-diindolylmethane, we found that survivin is playing an important role during 3,3′-diindolylmethane-induced cell death.

Our results also showed that cyclins (cyclin A2 and cyclin E2) and CDCs (cdc25A and cdc45) were down-regulated in 3,3′-diindolylmethane-treated breast cancer cells, whereas CDK inhibitors (p21^{WAF1} and p57) were up-regulated, suggesting that 3,3′-diindolylmethane inhibited the growth of breast cancer cell through the arrest of cell cycle and inhibition of proliferation (Fig. 4). Similar effects on the cell cycle were also observed in

Table 2. The primer used for real-time RT-PCR analysis

Genes	Primer sequence
CCNE2	GAATGTCAAGACGAAGTA
	ATGAACATATCTGCTCTC
cdc25A	ACACAGCAACTAGCCATCTCCAG
	GCCAGCCTCCTTACCATCACG
MCM5	GACCATCTCTATCGCCAAG
	CTCCTCATTGTGCTCATCC
BIRC5	GCTTTCAGGTGCTGGTAG
	GATGTGGATCTCGGCTTC
PCNA	CCTGTAGCGGCGTTGTTG
	CGTTGATGAGGTCCTTGAGTG
Aik2	ACTTCGGCTGGTCTGTCC
	ATAGGTCTCGTTGTGTGATGC
p57^{Kip2}	GGACGAGACAGGCGAACC
	AGAGGACAGCGAGAAGAAGG
p21^{Cip1}	TCCAGCGACCTTCCTCATCCAC
	TCCATAGCCTCTACTGCCACCATC
UBCH10	TAGGAGAACCCAACATTGATA
	AGACGACACAAGGACAGG
FOXM1	AACCGCTACTTGACATTGG
	GCAGTGGCTTCATCTTCC
E2F1	CAAGAAGTCCAAGAACCACATCC
	CTGCTGCTCGCTCTCCTG
BACH1	TTTGGGACACGCACACAC
	ACCGACTACCTCAGGATGG
CTGF	ACCAATGACAACGCCTCCTG
	TTGCCCTTCTTAATGTTCTCTTCC
TACC3	ATCGTCTGTTCTTCGTGTG
	AGTCCAAGGGTGTCATCC
β-Actin	CCACACTGTGCCCATCTACG
	AGGATCTTCATGAGGTAGTCAGTCAG

3,3′-diindolylmethane-treated prostate cancer cells (3). Several studies have shown that CDCs control the molecules related to the cell cycle, and they are vital and important for the initiation and progression of the consecutive phase of the cell cycle (31, 32). It has been found that cyclins binds to cyclin-dependent protein kinase (CDK) and CDCs to control the cell cycle process (33–36). The CDK inhibitors, including p21^{WAF1}, p27, and p57, have been shown to arrest the cell cycle and inhibit the growth of cancer cells (37–39). Inhibition of cell growth by 3,3′-diindolylmethane could also be due to the induction of apoptosis in addition to cell cycle arrest. Moreover, after analyzing microarray data, we focused on determining whether 3,3′-diindolylmethane could induce apoptosis by inhibiting the expression of survivin, which may be critically important for cell survival and cell death.

Survivin is an IAP, which is overexpressed in human cancer cells and critically needed for regulation of the balance among cell proliferation, differentiation, and apoptosis (17). It is known that nuclear factor-κB (NF-κB), a key transcription factor, up-regulates the expression and function of survivin in breast cancer cells (40). It has also been shown that expression of antiapoptotic protein

survivin is associated with cancer cell viability and drug resistance (10). Previous studies in determining the association of survivin with prognosis in breast cancer patients has been controversial (17); thus, the clinical importance of survivin expression remains unclear in patients with breast cancer. However, down-regulation of survivin signaling may be a novel approach in breast cancer therapy. Because of the critical role of survivin in cell proliferation and apoptosis, we explored whether survivin could be a molecular target for 3,3′-diindolylmethane-induced cell growth inhibition and apoptosis. In this study, we showed, for the first time that 3,3′-diindolylmethane down-regulates survivin expression along with other antiapoptotic molecules. We also found that down-regulation of survivin by siRNA together with 3,3′-diindolylmethane treatment caused cell growth inhibition and apoptosis to a greater degree in breast cancer cells compared with either agent alone. Over-expression of survivin by survivin cDNA transfection abrogated 3,3′-diindolylmethane-induced apoptosis to certain degree. Therefore, we strongly believe that down-regulation of survivin is mechanistically linked with 3,3′-diindolylmethane-induced cell growth inhibition and apoptosis.
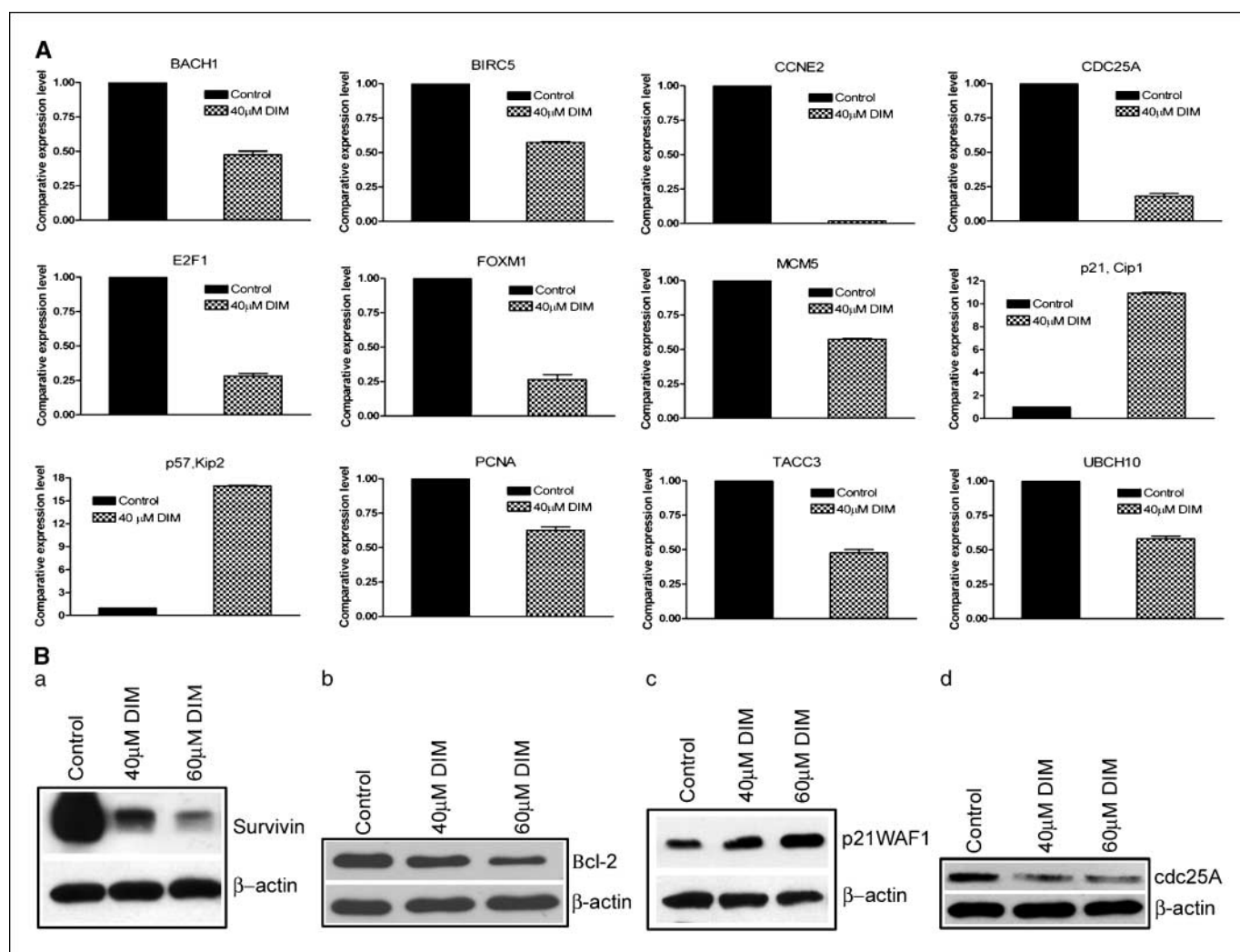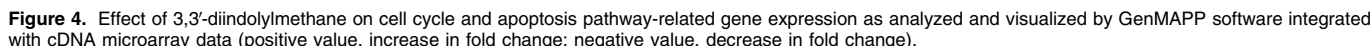

Figure 3. *A,* real-time RT-PCR amplification value showing the altered expression of specific genes from RNA of 3,3′-diindolylmethane (*DIM*)–treated MDA-MB-231 cells. *B,* Western blot analysis of selected gene expression in 3,3′-diindolylmethane-treated MDA-MB-231 cells at the protein level. *a,* expression of survivin was down-regulated with 3,3′-diindolylmethane treatment. *b,* expression of Bcl-2 was down-regulated with 3,3′-diindolylmethane treatment. *c,* expression of p21^{WAF1} was up-regulated with 3,3′-diindolylmethane treatment. *d,* expression of cdc25A was down-regulated with 3,3′-diindolylmethane treatment.

Figure 4. Effect of 3,3′-diindolylmethane on cell cycle and apoptosis pathway-related gene expression as analyzed and visualized by GenMAPP software integrated with cDNA microarray data (positive value, increase in fold change; negative value, decrease in fold change).

It has been reported that ectopic expression of survivin, an inhibitor of apoptosis, confers resistance to apoptosis to a variety of stimuli, and survivin is one of the most abundantly overexpressed genes in human tumors (41, 42). Genetic and biochemical data indicate that survivin functions in a unique cell division checkpoint that ensures the apoptotic demise of genetically unstable cells (41). Based on these findings, survivin has been proposed as a suitable target for drugs that can restore the apoptotic program in human tumors. A recent study has indicated that anti-survivin oligonucleotides induced apoptosis in mesothelinoma cells, suggesting that down-regulation of survivin seems to be an effective therapy for mesothelioma (42). Another study has shown that survivin is expressed in the G_2-M phase of the cell cycle in a cycle-regulated manner (41). It has been shown that GADD45A promotes apoptosis and regulates G_2-M arrest (43), and in our study, we found that GADD45A and FOXO3A expression was up-regulated by 3,3′-diindolylmethane treatment, which could be associated with apoptotic mechanisms (44, 45). Induction of apoptosis by FOXO3A has been correlated with the disruption of mitochondrial member integrity, cytochrome *c* release, and up-regulation of BIM (46). The induction of apoptosis mediated by these molecules, including survivin, could be important molecular mechanism(s) by which 3,3′-diindolylmethane exerts its growth-inhibitory effects on breast cancer cells.
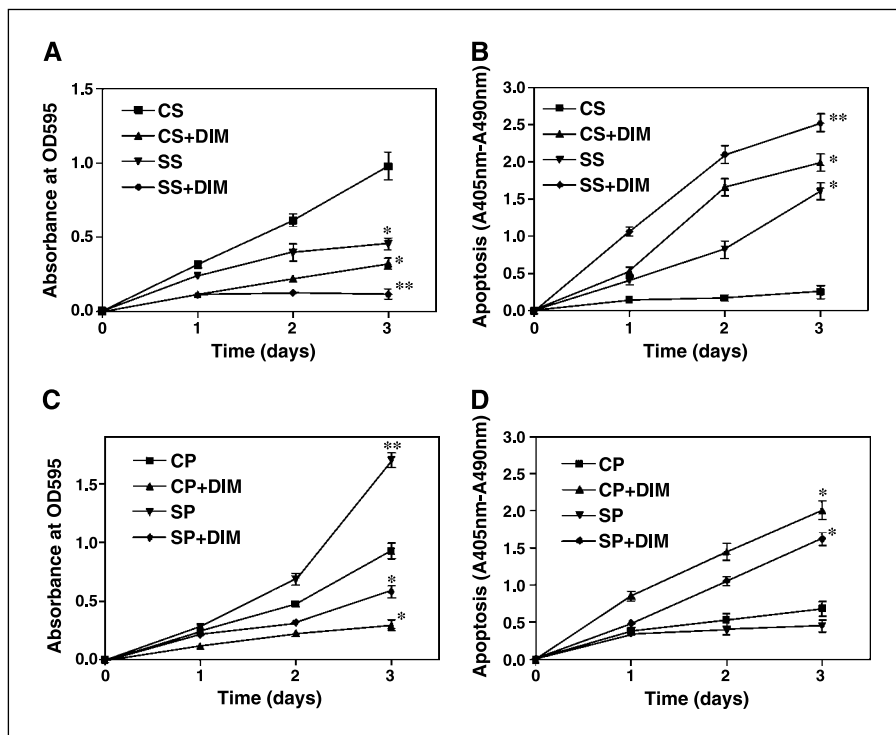
We also found that 3,3′-diindolylmethane down-regulated the expression of the forkhead transcription factor FOXM1, which correlates with proliferative status in a variety of normal and transformed cell types (47). Elevated expression of FOXM1 has been noted in both hepatocellular carcinoma and basal cell carcinoma (47). It has been indicated that FOXM1 is significantly elevated in primary breast cancer (47). Our microarray analysis showed that FOXM1 regulates genes, including *survivin*, that are essential for mitosis. Loss of FOXM1 expression generates mitotic spindle defects, delays cells in mitosis, and induces mitotic catastrophe (47). At the beginning of mitosis, survivin associates

Figure 5. MDA-MB-231 breast cancer cell growth inhibition and cell death induced by survivin siRNA and 3,3′-diindolylmethane. Survivin expression was down-regulated by 3,3′-diindolylmethane and survivin siRNA, resulting in cell death.

Figure 6. MDA-MB-231 breast cancer cell growth inhibition and cell death by survivin cDNA, survivin siRNA, and 3,3'-diindolylmethane (*DIM*). CS, control siRNA; SS, survivin siRNA; CP, control plasmid; SP, survivin plasmid. *A*, down-regulation of survivin expression significantly inhibited cell growth. 3,3'-Diindolylmethane plus survivin siRNA inhibited cell growth to a greater degree compared with 3,3'-diindolylmethane or survivin alone. *B*, MDA-MB-231 breast cancer cell death induced by survivin siRNA and 3,3'-diindolylmethane. Down-regulation of survivin expression significantly increased apoptosis induced by 3,3'-diindolylmethane. Survivin siRNA–transfected MDA-MB-231 cells were significantly more sensitive to spontaneous and 3,3'-diindolylmethane-induced apoptosis. *C*, overexpression of survivin expression significantly promoted cell growth. Overexpression in survivin rescued breast cancer cells from 3,3'-diindolylmethane-induced cell growth inhibition. *D*, overexpression of survivin by survivin cDNA transfection abrogated 3,3'-diindolylmethane-induced apoptosis. *, $P < 0.05$; **, $P < 0.01$.

with microtubules of the mitotic spindle on a specific and saturable reaction that is regulated by microtubule dynamics (48). Our present findings indicated that inhibition of FOXM1 expression by 3,3'-diindolylmethane, which may disrupt survivin-microtubule interactions, resulted in the loss of survivin's antiapoptosis function and increased caspase-3 activity, a mechanism involved in cell death during mitosis. In contrast, 3,3'-diindolylmethane up-regulated the expression of tumor-suppressor genes, including *p21^{WAF1}* and *p57*, which may inhibit survivin expression. These results are novel and suggest that 3,3'-diindolylmethane may induce the apoptotic pathway by inhibiting cancer cell growth and survival through inhibition of transcription and oncogenesis (hypothetical diagram as in Fig. 7).

Several other potential mechanisms could explain the regulation of survivin associated with inhibition of cell proliferation and

induction of apoptosis. It is known that NF-κB, a transcription factor, plays important roles in the control of cell growth, differentiation, and apoptosis (11, 12, 14, 16, 49, 50). Several studies have suggested that the activation of NF-κB up-regulates the expression of its downstream genes, such as *Bcl-2/Bcl-X_L* and *survivin*, which are involved in cancer cell invasion, metastasis, and resistance to chemotherapy (16, 51). We have previously found that 3,3'-diindolylmethane is a potent inhibitor of NF-κB DNA-binding activity in breast cancer cells (8). Thus, 3,3'-diindolylmethane induced down-regulation of survivin expression could be partly due to inhibition of NF-κB activity (hypothetical diagram as in Fig. 7). We, therefore, believe that 3,3'-diindolylmethane could inhibit NF-κB expression, resulting in the down-regulation of its target genes, including *survivin*, and causing cell growth inhibition and apoptosis.

Taken together, we believe that targeting survivin by 3,3'-diindolylmethane could be a novel approach for the prevention and/or treatment of breast cancer. Moreover, the down-regulation of survivin by 3,3'-diindolylmethane could also be a useful strategy for chemosensitization of metastatic breast cancer cells to standard therapies. However, further in-depth investigations are needed to establish the cause and effect relationship of *survivin* gene regulation and 3,3'-diindolylmethane-induced cell growth inhibition and apoptosis in breast cancer in animal and human models.

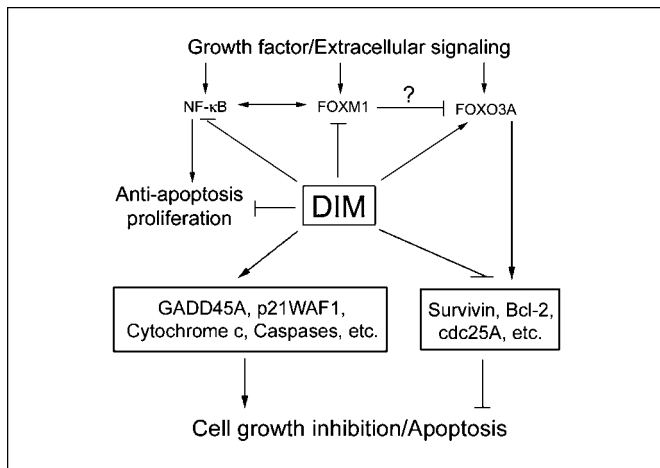**Figure 7.** A schematic representation showing 3,3'-diindolylmethane(*DIM*)–induced cell growth inhibition and apoptosis in breast cancer cells.

Acknowledgments

References

1. Seymour JD, Calle EE, Flagg EW, Coates RJ, Ford ES, Thun MJ. Diet Quality Index as a predictor of short-term mortality in the American Cancer Society Cancer Prevention Study II Nutrition Cohort. Am J Epidemiol 2003;157:980–8.
2. Li Y, Che M, Bhagat S, et al. Regulation of gene expression and inhibition of experimental prostate cancer bone metastasis by dietary genistein. Neoplasia 2004;6:354–63.
3. Li Y, Li X, Sarkar FH. Gene Expression profiles of I3C- and DIM-treated PC3 human prostate cancer cells determined by cDNA microarray analysis. J Nutr 2003;133:1011–9.
4. Rahman KM, Li Y, Sarkar F. Inactivation of Akt and NF-kB play important roles during I3C-induced apoptosis in breast cancer cells. Nutr Cancer 2004;48:84–94.
5. Rahman KM, Aranha O, Glazyrin A, Chinni SR, Sarkar FH. Translocation of Bax to mitochondria induces apoptotic cell death in indole-3-carbinol (I3C) treated breast cancer cells. Oncogene 2000;19:5764–71.
6. Rahman KM, Sarkar FH. Steroid hormone mimics: molecular mechanisms of cell growth and apoptosis in normal and malignant mammary epithelial cells. J Steroid Biochem Mol Biol 2002;80:191–201.
7. Rahman KM, Aranha O, Sarkar FH. Indole-3-carbinol (I3C) induces apoptosis in tumorigenic but not in nontumorigenic breast epithelial cells. Nutr Cancer 2003;45:101–12.
8. Rahman KM, Sarkar FH. Inhibition of nuclear translocation of nuclear factor-{kappa}B contributes to 3,3′-diindolylmethane-induced apoptosis in breast cancer cells. Cancer Res 2005;65:364–71.
9. Tsuji N, Furuse K, Asanuma K, et al. Mutations of the p53 gene and loss of heterozygosity at chromosome 17p13.1 are associated with increased survivin expression in breast cancer. Breast Cancer Res Treat 2004;87:23–31.
10. Wu J, Ling X, Pan D, et al. Molecular mechanism of inhibition of survivin transcription by the GC-rich sequence selective DNA-binding antitumor agent, hedamycin: evidence of survivin downregulation associated with drug sensitivity. J Biol Chem 2005;280:9745–51.
11. Biswas DK, Dai SC, Cruz A, Weiser B, Graner E, Pardee AB. The nuclear factor kappa B (NF-kappa B): a potential therapeutic target for estrogen receptor negative breast cancers. Proc Natl Acad Sci U S A 2001;98:10386–91.
12. Hideshima T, Chauhan D, Richardson P, et al. NF-kappa B as a therapeutic target in multiple myeloma. J Biol Chem 2002;277:16639–47.
13. Ikeguchi M, Kaibara N. Changes in survivin messenger RNA level during cisplatin treatment in gastric cancer. Int J Mol Med 2001;8:661–6.
14. Orlowski RZ, Baldwin AS, Jr. NF-kappaB as a therapeutic target in cancer. Trends Mol Med 2002;8:385–9.
15. Zhang SQ, Qiang SY, Yang WB, Jiang JT, Ji ZZ. Expression of survivin in different stages of carcinogenesis and progression of breast cancer. Ai Zheng 2004;23:697–700.
16. Haefiner B. Nf-kappaB: arresting a major culprit in cancer. Drug Discov Today 2002;7:653–63.

17. Span PN, Sweep FC, Wiegerinck ET, et al. Survivin is an independent prognostic marker for risk stratification of breast cancer patients. Clin Chem 2004;50:1986–93.
18. Ashok BT, Chen YG, Liu X, et al. Multiple molecular targets of indole-3-carbinol, a chemopreventive anti-estrogen in breast cancer. Eur J Cancer Prev 2002;11 Suppl 2:S86–93.
19. Chang X, Tou JC, Hong C, et al. 3,3′-Diindolylmethane inhibits angiogenesis and the growth of transplantable human breast carcinoma in athymic mice. Carcinogenesis 2005;26:771–8.
20. Hong C, Firestone GL, Bjeldanes LF. Bcl-2 family-mediated apoptotic effects of 3,3′-diindolylmethane (DIM) in human breast cancer cells. Biochem Pharmacol 2003;65:1085–97.
21. Hong C, Kim HA, Firestone GL, Bjeldanes LF. 3,3′-Diindolylmethane (DIM) induces a G(1) cell cycle arrest in human breast cancer cells that is accompanied by Sp1-mediated activation of p21(WAF1/CIP1) expression. Carcinogenesis 2002;23:1297–305.
22. Howells LM, Gallacher-Horley B, Houghton CE, Manson MM, Hudson EA. Indole-3-carbinol inhibits protein kinase B/Akt and induces apoptosis in the human breast tumor cell line MDA MB468 but not in the nontumorigenic HBL100 line. Mol Cancer Ther 2002;1:1161–72.
23. Kudoh K, Ramanna M, Ravatn R, et al. Monitoring the expression profiles of doxorubicin-induced and doxorubicin-resistant cancer cells by cDNA microarray. Cancer Res 2000;60:4161–6.
24. Zembutsu H, Ohnishi Y, Tsunoda T, et al. Genome-wide cDNA microarray screening to correlate gene expression profiles with sensitivity of 85 human cancer xenografts to anticancer drugs. Cancer Res 2002;62:518–27.
25. Anderton MJ, Jukes R, Lamb JH, et al. Liquid chromatographic assay for the simultaneous determination of indole-3-carbinol and its acid condensation products in plasma. J Chromatogr B Analyt Technol Biomed Life Sci 2003;787:281–91.
26. Shilling AD, Carlson DB, Katchamart S, Williams DE. 3,3′-diindolylmethane, a major condensation product of indole-3-carbinol, is a potent estrogen in the rainbow trout. Toxicol Appl Pharmacol 2001;170:191–200.
27. Sizemore N, Leung S, Stark GR. Activation of phosphatidylinositol 3-kinase in response to interleukin-1 leads to phosphorylation and activation of the NF-kappaB p65/RelA subunit. Mol Cell Biol 1999;19:4798–805.
28. Stresser DM, Blanchard AP, Turner SD, et al. Substrate-dependent modulation of CYP3A4 catalytic activity: analysis of 27 test compounds with four fluorometric substrates. Drug Metab Dispos 2000;28:1440–8.
29. Eisen MB, Spellman PT, Brown POBotstein D. Cluster analysis and display of genome-wide expression patterns. Proc Natl Acad Sci U S A 1998;95:14863–8.
30. Khatri P, Draghici S, Ostermeier GC, Krawetz SA. Profiling gene expression using onto-express. Genomics 2002;79:266–70.
31. Nilsson I, Hoffmann I. Cell cycle regulation by the Cdc25 phosphatase family. Prog Cell Cycle Res 2000;4:107–14.
32. Poggioli GJ, Dermody TS, Tyler KL. Reovirus-induced sigma1s-dependent G(2)/M phase cell cycle arrest is

associated with inhibition of p34(cdc2). J Virol 2001;75:7429–34.
33. Brechot C. Oncogenic activation of cyclin A. Curr Opin Genet Dev 1993;3:11–8.
34. Erlanson M, Landberg G. Prognostic implications of p27 and cyclin E protein contents in malignant lymphomas. Leuk Lymphoma 2001;40:461–70.
35. Obaya AJ, Sedivy JM. Regulation of cyclin-Cdk activity in mammalian cells. Cell Mol Life Sci 2002;59:126–42.
36. Sherr CJ. D-type cyclins. Trends Biochem Sci 1995;20:187–90.
37. el-Deiry WS, Tokino T, Waldman T, et al. Topological control of p21$^{WAF1/CIP1}$ expression in normal and neoplastic tissues. Cancer Res 1995;55:2910–9.
38. Kawamata N, Morosetti R, Miller CW, et al. Molecular analysis of the cyclin-dependent kinase inhibitor gene p27/Kip1 in human malignancies. Cancer Res 1995;55:2266–9.
39. Kobatake T, Yano M, Toyooka S, et al. Aberrant methylation of p57KIP2 gene in lung and breast cancers and malignant mesotheliomas. Oncol Rep 2004;12:1087–92.
40. Chen X, Kandasamy K, Srivastava RK. Differential roles of RelA (p65) and c-Rel subunits of nuclear factor kappa B in tumor necrosis factor-related apoptosis-inducing ligand signaling. Cancer Res 2003;63:1059–66.
41. Li F, Ambrosini G, Chu EY, et al. Control of apoptosis and mitotic spindle checkpoint by survivin. Nature 1998;396:580–4.
42. Xia C, Xu Z, Yuan X, et al. Induction of apoptosis in mesothelioma cells by antisurvivin oligonucleotides. Mol Cancer Ther 2002;1:687–94.
43. Maeda T, Hanna AN, Sim AB, Chua PP, Chong MT, Tron VA. GADD45 regulates G_2/M arrest, DNA repair, and cell death in keratinocytes following ultraviolet exposure. J Invest Dermatol 2002;119:22–6.
44. Schmidt M, Fernandez de Mattos S, van der Horst A, et al. Cell cycle inhibition by FoxO forkhead transcription factors involves downregulation of cyclin D. Mol Cell Biol 2002;22:7842–52.
45. Yakirevich E, Maroun L, Cohen O, Izhak OB, Rennert G, Resnick MB. Apoptosis, proliferation, and Fas (APO-1, CD95)/Fas ligand expression in medullary carcinoma of the breast. J Pathol 2000;192:166–73.
46. Stahl M, Dijkers PF, Kops GJ, et al. The forkhead transcription factor FoxO regulates transcription of p27Kip1 and Bim in response to IL-2. J Immunol 2002;168:5024–31.
47. Wonsey DR, Follettie MT. Loss of the forkhead transcription factor FoxM1 causes centrosome amplification and mitotic catastrophe. Cancer Res 2005;65:5181–9.
48. Hirokawa N. Microtubule organization and dynamics dependent on microtubule-associated proteins. Curr Opin Cell Biol 1994;6:74–81.
49. Bharti AC, Aggarwal BB. Chemopreventive agents induce suppression of nuclear factor-kappaB leading to chemosensitization. Ann N Y Acad Sci 2002;973:392–5.
50. Bharti AC, Aggarwal BB. Nuclear factor-kappa B and cancer: its role in prevention and therapy. Biochem Pharmacol 2002;64:883–8.
51. Clark AS, West K, Streicher S, Dennis PA. Constitutive and inducible Akt activity promotes resistance to chemotherapy, trastuzumab, or tamoxifen in breast cancer cells. Mol Cancer Ther 2002;1:707–17.

Therapeutic intervention of experimental breast cancer bone metastasis by indole-3-carbinol in SCID-human mouse model

KM Wahidur Rahman,[1] Fazlul H. Sarkar,[1] Sanjeev Banerjee,[1] Zhiwei Wang,[1] Dezhong J. Liao,[1] Xin Hong,[1] and Nurul H. Sarkar[2]

[1]Department of Pathology, Karmanos Cancer Institute, Wayne State University School of Medicine, Detroit, Michigan and [2]Institute of Molecular Medicine and Genetics, Medical College of Georgia, Augusta, Georgia

Abstract

Several lines of experimental evidence have suggested that chemokine receptor CXCR4, a metastasis-promoting molecule, may play important roles in breast cancer bone metastasis. There is emerging evidence linking CXCR4 to matrix metalloproteinases (MMP) as well as their regulator nuclear factor-κB (NF-κB), a key transcription factor, which is known to activate metastasis-promoting molecules for many types of malignancies, including breast cancer. A recent study also showed that promoter region of CXCR4 has several NF-κB-binding sites, suggesting that there may be a cross-talk between CXCR4 and NF-κB. We have shown previously that indole-3-carbinol (I3C), a natural compound present in vegetables of the genus *Brassica*, can inhibit NF-κB in breast cancer cells. However, there are no reports in the literature showing any effect of I3C on CXCR4 expression *in vitro* and *in vivo*. We therefore examined whether I3C could inhibit bone metastasis of breast cancer by inhibiting CXCR4 and MMP-9 expression mediated via the inhibition of the NF-κB signaling pathway. Here, we have modified the severe combined immunodeficient (SCID)-human mouse model of experimental bone metastasis for use with the MDA-MB-231 breast cancer cell line. In this animal model, we found that I3C significantly inhibited MDA-MB-231 bone tumor growth, and our results were correlated with the down-regulation of NF-κB. Moreover, we found that I3C significantly inhibited the expression of multiple genes involved in the control of metastasis and invasion *in vitro* and *in vivo*, especially the expression of CXCR4 and MMP-9 along with pro-MMP-9, with concomitant decrease in Bcl-2 and increase in the proapoptotic protein Bax. From these results, we conclude that the CXCR4/NF-κB pathway is critical during I3C-induced inhibition of experimental breast cancer bone metastasis. These results also suggest that I3C could be a promising agent for the prevention and/or treatment of breast cancer bone metastasis in the future. [Mol Cancer Ther 2006;5(11):2747–56]

Introduction

Metastasis is a nonrandom process, and each cancer type has its own preferred sites of metastasis (1, 2). Metastasis of cancer cells is a complex process involving multiple steps, including invasion, angiogenesis, intravasation, trafficking of cancer cells through blood vessels, extravasations, organ-specific homing, and growth (3, 4). Bone is one of the most common sites of metastasis for human breast cancer (5). A recent study has shown that a chemokine receptor, CXCR4, is highly expressed in breast cancer cells but not in normal breast tissue, whereas its ligand, stromal-derived factor-1α (SDF-lα; also called CXCL12), is expressed in those organs where breast cancer metastasis is frequently found (6). Thus, it is quite possible that CXCR4 and/or SDF-1α signaling may be involved in attracting and homing breast cancer cells in the bone.

There are some protease systems that are required for extracellular matrix degradation for the growth of cancer cells at the metastatic sites. Matrix metalloproteinases (MMP) are a group of enzymes required for extracellular matrix degradation for the growth of cancer cells at the metastatic sites (3, 4). These enzymes are secreted as pro-proteins and usually need to be activated by urokinase-type plasminogen activators (uPA; 3, 4). There is increasing evidence connecting CXCR4 to MMPs, IL-8, and uPA (7). MMPs and uPA as well as their regulator nuclear factor-κB (NF-κB), a key transcription factor, are known to activate metastasis-promoting molecules for many types of malignancies, including breast cancer (5, 6, 8–13). NF-κB was also found to be constitutively activated in human breast cancer (14, 15). A recent study and TESS analysis (TRANSFAC 4.0 database version) also showed that the promoter region of CXCR4 has several NF-κB-binding sites, suggesting that there may be a cross-talk between NF-κB and CXCR4 (16–18). Thus, NF-κB may regulate the expression and function of CXCR4, which may, in part, be activated via up-regulation of the expression of IL-8, uPA, and MMP-9 (19). Taken together, CXCR4 may be the point of convergence of many mediators of metastatic processes at the metastatic sites.

Indole-3-carbinol (I3C) and its stable condensation product, 3,3′-diindolylmethane, are compounds that are abundant

---

in cruciferous vegetables and have been shown to possess inhibitory effects on the growth and metastatic abilities of several prostate and breast cancer cell lines (20–29). It has also been shown that I3C and 3,3′-diindolylmethane inhibit cell growth and induce apoptotic cell death by their pleiotropic effects on the regulation of multiple genes, such as *p21, p27, cyclin-dependent kinase, survivin, Bax/Bcl-2, cytochrome P450 1A1*, and *GADD153* (28, 30). Interestingly, our recent studies have shown that the effect of I3C and 3,3′-diindolylmethane is mediated by the inactivation of NF-κB (23–27, 29). Thus, agents that directly block the expression of CXCR4 signaling, partly due to inhibition of NF-κB, may have great therapeutic potential for treating metastatic breast cancer. I3C also inhibits the *in vitro* invasive potential of human breast cancer cell lines, suggesting that I3C could inhibit the metastatic growth of breast cancer (31). Collectively, these studies suggest that NF-κB may play a pivotal role in controlling breast cancer metastasis, a concept supported by many other lines of evidence, in breast cancer and other types of malignancies (23–27, 29). We report here that I3C treatment of MBA-MB-231 breast cancer cells results in decreased CXCR4 mRNA expression. However, the role of I3C in the inhibition of bone metastasis of human breast cancer has not been documented, perhaps due to a lack of appropriate animal models of experimental breast cancer bone metastasis. We hypothesize that I3C-induced inhibition of NF-κB will inhibit CXCR4 and other NF-κB targeted genes that could be mechanistically responsible for the inhibition of experimental breast cancer bone metastasis in a suitable animal model.

There are some reports in the literature about the spontaneous animal model of breast cancer (32, 33). A mouse model of human prostate cancer metastasis [severe combined immunodeficient (SCID)−human (SCID-hu)] using human prostate cancer cells grown in the human bone implanted into SCID mice has been developed by Nemeth et al. (34). But there are no other reports in the literature about suitable animal models that could be used faithfully for studying human breast cancer bone metastasis using human breast cancer cell lines that grow in the marrow of human bone environment implanted s.c. into mice. We believe that the advantage of SCID-hu model may provide a more clinically relevant model for growth of human breast cancer in a human bone microenvironment. For these reasons, here, we have adapted the SCID-hu model of experimental bone metastasis for use with the MDA-MB-231 breast cancer cell line and determined the effect of I3C *in vivo* in this model to test our hypothesis as stated above. We found that I3C could inhibit the growth of MDA-MB-231 cells in a SCID-hu model with concomitant inhibition of CXCR4, MMP-9, and Bcl-2 mediated by the down-regulation of NF-κB.

Materials and Methods

Two-Step Real-time Quantitative Reverse Transcription-PCR Analysis of Gene Expression in I3C-Treated MDA-MB-231 Breast Cancer Cells

Total RNA was isolated in I3C-treated MDA-MB-231 breast cancer cell line by Trizol (Invitrogen, Carlsbad, CA). One microgram of total RNA was subjected to first-strand cDNA synthesis using Taqman reverse transcription reagents kit (Applied Biosystems, Foster City, CA) in a total volume of 50 μL, including 6.25 units MultiScribe reverse transcriptase and 25 pmol random hexamers. Reverse transcription reaction was done with 25°C for 10 minutes followed by 48°C for 30 minutes and 95°C for 5 minutes. The primers were checked by running a virtual PCR, and primer concentration was optimized to avoid primer dimer formation. In addition, dissociation curves were checked to avoid nonspecific amplification. Real-time PCR amplications were undertaken in Mx4000 Multiplex QPCR System (Stratagene, La Jolla, CA) using 2 × SYBR Green PCR Master Mix (Applied Biosystems). One microliter reverse transcriptase reaction was used for a total volume of 25 μL quantitative PCRs. The thermal profile for SYBR real-time PCR was 95°C for 10 minutes followed by 40 cycles of 95°C for 15 seconds and 60°C for 1 minute.

Animal Care and Human Bone Implantation

Female homozygous CB17 scid/scid mice, ages 4 weeks, were purchased from Taconic Farms (Germantown, NY). The mice were maintained according to the NIH standards established in the "Guidelines for the Care and Use of Experimental Animals," and all experimental protocols were approved by the Animal Investigation Committee of Wayne State University (Detroit, MI). Human fetal bone tissue was obtained by a third party, nonprofit organization (Advanced Bioscience Resources, Alameda, CA), and written informed consent was obtained from the donor, consistent with regulations issued by each state involved and the federal government. Human fetal femurs and humeri of 16 to 22 weeks of development were divided in half longitudinally and then again in half transversely into four fragments ∼1 cm long and 3 or 4 mm in diameter (34). After 1 week of acclimatization, these bone fragments were implanted s.c. in the flank through a small skin incision with the opened marrow cavity against the mouse muscle. Isoflurane anesthesia was used during all surgical procedures.

Production of Breast Cancer Bone Tumors and I3C Treatment

Suspensions of MDA-MB-231 cells (2×10^5 cells in a volume of 20 μL PBS) were injected using a 27-gauge needle through the mouse skin directly into the marrow of implanted fetal bone. The mice were then divided into two groups: control ($n = 10$) and intervention ($n = 10$) groups (Fig. 2). Sesame seed oil was used to facilitate gavage and avoid irritation of the esophagus and was safe as shown also by others (35, 36). The mice in the intervention group were given I3C (1 mg/d/mouse) by oral gavage everyday for 5 weeks as soon as the majority of the bone implants began to enlarge (now called a "bone tumor") as determined by caliper measurements (23rd day after cancer cell injection). The control mice received only sesame seed oil without I3C. The volume of the bone tumor in each group was determined by twice-weekly caliper measurements according to the formula $ab^2 / 2$, where a is the length and b is the

shortest measurement. Percentage (%) reduction in tumor volume at the end of the treatment was deduced by the formula: volume of tumor in experimental group / volume in control mice × 100. The statistical significance of differential findings between the experimental groups and control was determined by Student's *t* test as implemented by Excel 2000 (Microsoft Corp., Redmond, WA). The mice were sacrificed 3 months after cell injection. Bone tumors were subjected to *ex vivo* imaging on a Lo-Rad M-IV mammography unit (Karmanos Cancer Institute, Detroit, MI) using a magnified specimen technique. Images were developed using a Kodak 2000 screen and radiography film (Kodak, Rochester, NY). On sacrifice, tumor tissue from each mouse was harvested and cut into two pieces; one part was frozen for molecular analysis, and the other part of the tissue was fixed in formalin and embedded in paraffin for histologic evaluation and immunohistochemistry.

Tissue Collection, Fixation, and H&E Staining

Freshly harvested tumors grown in the implanted bones were fixed in 10% buffered formalin for 48 hours and decalcified with 10% EDTA, embedded, and sectioned. Samples were then washed with tap water and soaked in a graded series of 50%, 60%, 70%, 80%, and 90% ethanol for 30 minutes and then in 90% and 100% ethanol for 1 hour. They were then held in a solution of 100% ethanol and xylene at a 1:1 ratio for 30 minutes before being embedded in paraffin and held at 60°C for 1 hour to make paraffin blocks. Transverse sections (5 μm) were taken from the blocks and prepared for histochemical and immunohistochemical staining. H&E staining was used for histologic observation.

Electrophoretic Mobility Shift Assay for Measuring NF-κB Activity

MDA-MB-231 cells were plated at a density of 1×10^6 in 100-mm dishes and cultured for 24 hours. Subsequently, the cultures were treated with 60 and 100 μmol/L I3C or DMSO for 24, 48, and 72 hours. I3C (Sigma-Aldrich, St. Louis, MO) was dissolved in DMSO (final concentration, 0.1%) to make a 10 mmol/L stock solution and was added directly to the culture medium at different concentrations. Nuclear extracts were prepared from control and I3C-treated breast epithelial cells as previously described (25, 29, 37) and subjected to analysis for NF-κB DNA-binding activity as measured by electrophoretic mobility shift assay. Using frozen tumor tissue, nuclear proteins were also extracted as described previously (25, 29, 37). Briefly, tissues were minced and incubated on ice for 30 minutes in 0.5 mL ice-cold buffer A composed of 10 mmol/L HEPES (pH 7.9), 1.5 mmol/L KCl, 10 mmol/L MgCl$_2$, 0.5 mmol/L DTT, 10% NP40, 0.1% IGEPAL CA-630, and 0.5 mmol/L phenylmethylsulfonyl fluoride. The minced tissue was homogenized using a Dounce homogenizer (Kontes Co., Vineland, NJ) followed by centrifugation at 5,000 × *g* at 4°C for 10 minutes. The supernatant (cytosolic proteins) was collected for Western blot analysis and kept at −70°C until use. The crude nuclear pellet was suspended in 200 μL buffer B [20 mmol/L HEPES (pH 7.9), 25% glycerol, 1.5 mmol/L MgCl$_2$, 420 mmol/L NaCl, 0.5 mmol/L DTT, 0.2 mmol/L EDTA, 0.5 mmol/L phenylmethylsulfonyl fluoride, 4 μmol/L leupeptin] and

incubated on ice for 30 minutes. The suspension was centrifuged at 16,000 × *g* at 4°C for 30 minutes. The supernatant (nuclear proteins) was collected and kept at −70°C until use. The protein concentration was determined using bicinchoninic acid protein assay (Pierce Chemical Co., Rockford, IL). Electrophoretic mobility shift assay was done by preincubating 8.0 μg nuclear extract with a binding buffer containing 20% glycerol, 100 mmol/L MgCl$_2$, 2.5 mmol/L EDTA, 2.5 mmol/L DTT, 250 mmol/L NaCl, 50 mmol/L Tris-HCl, and 0.25 mg/mL poly(deoxyinosinic-deoxycytidylic acid) for 10 minutes. After the addition of IRDye 700-labeled NF-κB oligonucleotide, samples were incubated for an additional 20 minutes. The DNA-protein complexes were electrophoresed in an 8.0% native polyacrylamide gel and then visualized by Odyssey Infrared Imaging System using Odyssey Software Release 1.1.

Western Blot Analysis for Measuring the Protein Levels of Bcl-2, Bax, CXCR4, and MMP-9 Activity

MDA-MB-231 cells were plated on culture dishes and allowed to attach for 24 hours followed by the addition of 60 or 100 μmol/L I3C and incubated for 24, 48, and 72 hours. Control cells were incubated in the medium with DMSO for similar times. Total cell lysates were prepared using the method as described previously (25, 29, 37). Using frozen tumor tissue, nuclear proteins were extracted using the method as described previously (25, 29, 37). Briefly, tissues were minced and incubated on ice for 30 minutes in 0.5 mL ice-cold buffer A, composed of 10 mmol/L HEPES (pH 7.9), 1.5 mmol/L KCl, 10 mmol/L MgCl$_2$, 0.5 mmol/L DTT, 10% NP40, 0.1% IGEPAL CA-630, and 0.5 mmol/L phenylmethylsulfonyl fluoride. The minced tissue was homogenized using a Dounce homogenizer followed by centrifuging at 5,000 × *g* at 4°C for 10 minutes. The supernatant (cytosolic proteins) was collected for Western blot analysis. Protein content was quantified with a bicinchoninic acid protein assay, and equal amounts of proteins were resolved by 10%, 12%, and 14% SDS-PAGE. Immunoblot was done with antibodies to Bcl-2 (Calbiochem, La Jolla, CA), Bax and CXCR4 (Santa Cruz Biotechnology, Inc., Santa Cruz, CA), MMP-9 (Santa Cruz Biotechnology), and β-actin (Sigma-Aldrich). A representative blot from three independent experiments was presented.

Immunohistochemical Staining for CXCR4 and MMP-9

Freshly harvested tumors grown in the implanted bones were fixed in 10% buffered formalin, decalcified, embedded, and sectioned. The paraffin sections of tumor tissues were deparaffinized then rehydrated through a graded alcohol series. Slides were placed in 10 mmol/L citrate buffer (pH 6.0) and heated in a microwave for 3 minutes. Nonspecific sites were blocked by incubation with Superbloc (ScyTek, Logan, UT). Sections were incubated with antibodies to MMP-9 (Calbiochem) and CXCR4 followed by staining with appropriate horseradish peroxidase–conjugated secondary antibodies followed by color development. The stained slides were dehydrated and mounted in per mount and visualized using an Olympus microscope (Olympus, Center Valley, PA). Images were captured with an attached camera linked to a computer.
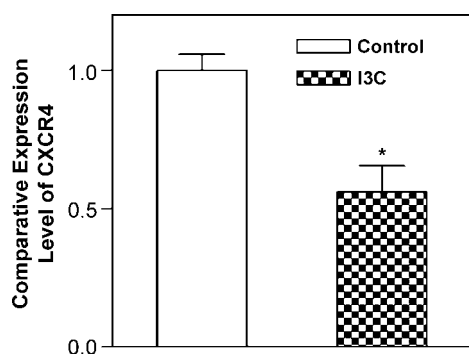
Figure 1. Real-time reverse transcription-PCR analysis of CXCR4 genes. Comparative analysis shows the down-regulation of CXCR4 mRNA expression in MDA-MB-231 cells grown in culture after 72 h of treatment with I3C compared with control. *, $P < 0.05$.

MMP-9 Activity Assay

MDA-MB-231 cells were seeded in a six-well plate (1.0×10^5 per well) and incubated at 37°C. After 24 hours, the complete medium was removed and the cells were washed with serum-free medium. The cells were then incubated in serum-free medium supplemented with 60 or 100 μmol/L I3C for 72 hours. MMP-9 activity in the conditioned medium and cell lysate was detected by using Fluorokine E Human MMP-9 Activity Assay kit (R&D System, Inc., Minneapolis, MN) according to the manufacturer's protocol.

Invasion Assay

The invasive activity of MDA-MB-231 cells with different treatments was tested by using BD BioCoat Tumor Invasion Assay System (BD Biosciences, Bedford, MA) according to the manufacturer's protocol with minor modification. Briefly, MDA-MB-231 cells (5×10^4) with serum-free medium supplemented with 60 or 100 μmol/L I3C were seeded into the upper chamber of the system. Bottom wells in the system were filled with complete medium and the same reagent treatment as the upper chamber. After 48 hours of incubation, the cells in the upper chamber were removed, and the cells, which invaded through the Matrigel matrix membrane, were stained with 4 μg/mL calcein AM in Hank's buffered saline at 37°C for 1 hour. Then, fluorescence of the invaded cells was read in ULTRA Multifunctional microplate reader (TECAN, Research Triangle Park, NC) at excitation/emission wavelengths of 530/590 nm. These fluorescently labeled invasive cells were also photographed under a fluorescent microscope.

Statistical Analysis

The statistical significance was determined using Student's *t* test, and $P < 0.05$ was considered significant.

Results

Regulation of CXCR4 mRNA Expression by I3C Treatment

A recent study has indicated that the MDA-MB-231 cell line highly expresses CXCR4 (17), and I3C has been shown to possess inhibitory effects on the growth and metastatic abilities of several cancers, including breast cancer (24–27, 29, 38–43). To confirm the alternations of CXCR4 expression after I3C treatment in MDA-MB-231 breast cancer cells, we conducted real-time reverse transcription-PCR analysis for the *CXCR4* gene (Fig. 1). The altered mRNA expression of CXCR4 was observed as early as 24 hours after I3C treatment and was significantly more evident after 72 hours treatment. The results of reverse transcription-PCR analysis for *CXCR4* gene along with published *in vitro* results suggest that I3C could regulate the transcription of genes involved in angiogenesis, tumor cell invasion, and metastasis (27–30, 38, 44–46). However, we asked the most important question whether I3C could affect tumor growth in the bone environment, which is answered by the following experiments.

Inhibition of Bone Tumor Growth by I3C

We report here, for the first time, the use of the SCID-hu animal model (34) as an experimental model for breast cancer bone metastasis and the effect of I3C *in vivo* in impeding tumor growth and metastasis. The experimental design and treatment schedule is depicted in Fig. 2. Currently, there are no reports in the literature documenting any effect of the host (i.e., mouse) environment on the bone xenograft (34, 47). Under our experimental conditions, administration of I3C by gavage treatment caused 50% reduction in tumor volume (Fig. 3A) compared with control group. The statistical analysis indicated that compared with the control group, bone tumor growth was significantly lower in the intervention ($P < 0.05$) group. The experiment was terminated 3 months after I3C treatment. We found that I3C (1 mg I3C/d/mouse) significantly inhibited breast cancer bone tumor growth (Fig. 3A and B) and osteolysis, documenting the efficacy of I3C in inhibiting breast cancer cell growth in the experimental model of bone metastasis. Figure 3B indicates *ex vivo* bone tumor X-ray showing bone osteolysis and
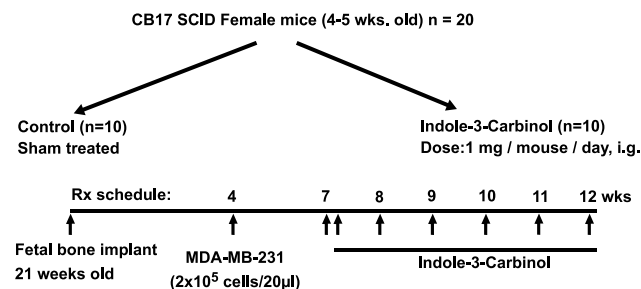

Figure 2. Flow chart representation of *in vivo* experimental design and treatment schedule. The human fetal bone was implanted s.c. in the right flank of female homozygous CB17 SCID mice through a small skin incision with the open marrow cavity against the mouse muscle. Four weeks after the bone implantation, suspensions of MDA-MB-231 cells (2×10^5 cells) were injected through the mouse skin directly into the marrow of implanted fetal bone. The mice in the intervention group were given I3C (1 mg/d/mouse) by oral gavage everyday for 5 wks as soon as the majority of the bone implants began to enlarge (now called a ''bone tumor'') as determined by caliper measurements (23rd day after cancer cell injection). The control mice received only saline without I3C. All animals were sacrificed at 12 wks after the start of the experiment.
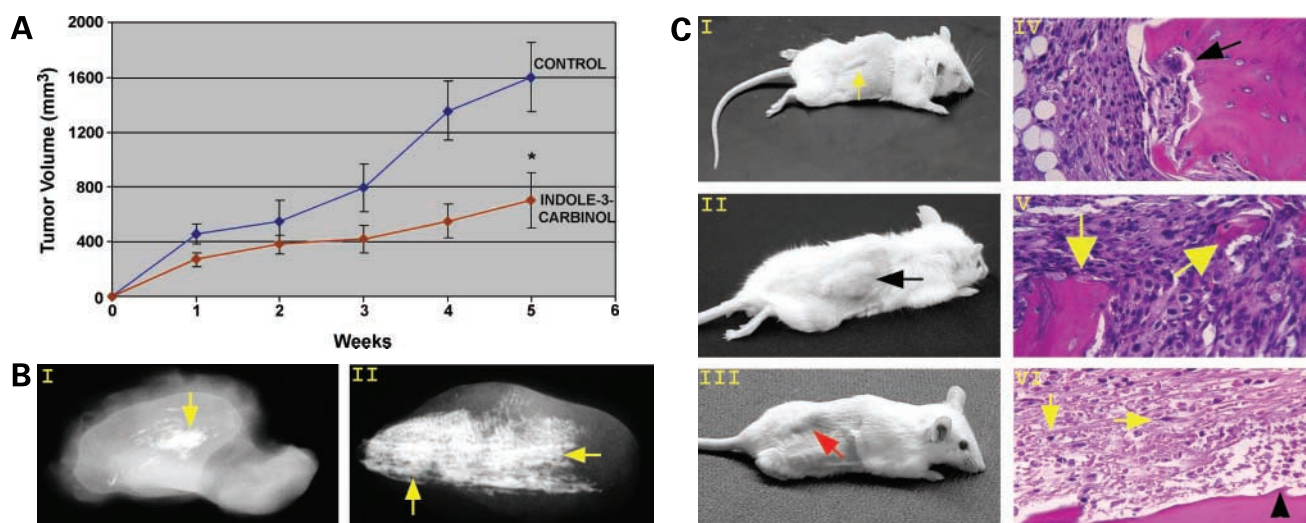
Figure 3. **A,** inhibitory effects of I3C on the growth of xenograft bone tumors of MDA-MB-231cells in SCID-hu mice. A total of 20 mice were divided into two groups. Under the experimental conditions, administration of I3C by gavage treatment caused 50% reduction in tumor volume compared with control group. *, $P < 0.05$. **B,** *ex vivo* bone tumor X-ray showing bone osteolysis and tumor growth of MDA-MB-231 cells in the control and I3C-treated group. *Arrow,* less residual bone in the control group (*I*) relative to I3C-treated group (*II*). We found that treatment with I3C inhibited tumor growth and osteolytic bone destruction resulting in more residual bone volume compared with control group (*I*). **C,** typical osteolytic bone metastasis of MDA-MB-231 cells in SCID-hu model. *I,* human fetal bone s.c. implanted in SCID mice. *II,* MDA-MB-231 cells (2×10^5) were injected directly into the marrow of implanted bone. *Black arrow,* the site of significant progression of tumor growth in representative untreated control mice. *III,* representative figure of mice from treatment group photographed at time of sacrifice showing significant regression of tumor growth (*red arrow*) by I3C treatment. *IV,* MDA-MB-231 cells were injected into the implanted human fetal bone showing invasion (*black arrow*). *V,* continuous osteolytic and invasive process resulting in gradual loss of the bone structure. *Yellow arrows,* residual bone surrounded by invasive tumor cells. *VI,* histologic evaluation showing I3C treatment resulted in pronounced death of tumor cells (*yellow arrows*) and preservation of the bone structure (*black arrowhead*).

tumor growth of MDA-MB-231 cells in the control and I3C treatment group. Arrow indicates less residual bone in the control group (Fig. 3B, *I*) relative to I3C-treated group (Fig. 3B, *II*). We found that treatment with I3C significantly inhibited cellular growth of breast cancer cells in a bone environment and also inhibited bone osteolysis in SCID-hu mice, showing an inhibitory effect of I3C in an *in vivo* model of experimental breast cancer bone metastasis. At autopsy, all tumors were found localized at the site of injection with essentially spread to no other organs. Our treatment conditions did not cause any weight loss of the animals, suggesting that I3C did not induce any deleterious effects under the present experimental conditions. These results show, for the first time, the efficacy of I3C in inhibiting tumor growth in an experimental breast cancer bone metastasis model.

Tumor Histology and Inhibition of Osteolysis by I3C

H&E histology evaluation showed typical osteolytic bone metastasis of MDA-MB-231 cells in SCID-hu animals (Fig. 3C). Human fetal bones s.c. implanted in SCID mice, as shown by representative figure, were randomly selected from each group (Fig. 3C, *I*). Suspensions of MDA-MB-231 cells (2×10^5 cells in a volume of 20 µL PBS) were injected using a 27-gauge needle through the mouse skin directly into the marrow of implanted fetal bone. Black arrow represents the site of significant progression of tumor growth as shown by representative figure from untreated group (Fig. 3C, *II*). Figure 3C (*III*) shows representative

figure of mice from treatment group photographed at the time of sacrifice. Red arrow represents the site of significant regression of tumor growth in I3C treatment group (Fig. 3C, *III*). In the control group, continuous osteolytic and invasive growth into the adjacent bone resulted in gradual loss of the bone structure (Fig. 3C, *IV, black arrow*). Yellow arrows indicate residual bone surrounded by invasive tumor cells (Fig. 3C, *V*). In contrast, the group receiving I3C treatment showed pronounced death of tumor cells (yellow arrows) and preservation of the bone structure (Fig. 3C, *VI, black arrowhead*). To further show whether the antitumor effect observed by I3C treatment could be due to inactivation of NF-κB, we did the following experiments.

Inhibition of NF-κB Activation by I3C

To answer the most important question, whether treatment of animals with I3C could effectively target a specific signaling molecule, such as NF-κB in tumor tissues, nuclear extract from frozen tumor tissues (randomly selected from control and treatment groups) was subjected to analysis for NF-κB DNA-binding activity as measured by electrophoretic mobility shift assay. The results are shown in Fig. 4B, which clearly show that I3C was effective in down-regulating NF-κB DNA-binding activity in animal tumors receiving I3C compared with control tumors. These *in vivo* results were similar to our *in vitro* findings (Fig. 4A), including our previously published data (27, 29), suggesting that the inactivation of NF-κB is at least one of the molecular mechanisms by which I3C induced antitumor activity in our
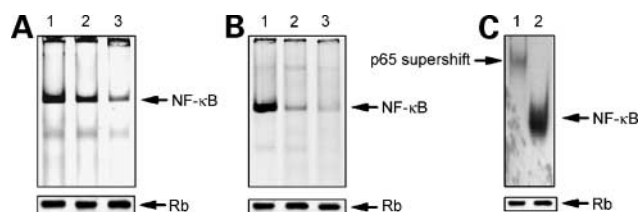
Figure 4. I3C abrogates NF-κB DNA-binding activity. **A,** I3C abrogates NF-κB DNA-binding activity in MDA-MB-231 breast cancer cells. Cells were treated with 60 or 100 μmol/L I3C (*lanes 2* and *3*, respectively) for 72 h. Nuclear extracts were prepared from control and I3C-treated cells and subjected to analysis for NF-κB DNA-binding activity as measured by electrophoretic mobility shift assay. **B,** MDA-MB-231 cells were grown in the marrow surface of the previously implanted bone in SCID animal. After the termination, tumors were removed and the nuclear proteins were subjected to analysis of the DNA-binding activity of NF-κB as measured by electrophoretic mobility shift assay. Gel shift assay for NF-κB done on randomly selected frozen tumor tissues obtained from each treatment groups of animals. Group 1 (*lane 1*, control animal; *lanes 2* and *3*, animal received I3C). Results showed that I3C was effective in down-regulating NF-κB in treated animals relative to control tumors. *Arrow,* NF-κB DNA-binding activity. **C,** the specificity of NF-κB DNA-binding activity was confirmed by supershift assays. Retinoblastoma (*Rb*) protein level served as nuclear protein loading control.

experimental animal model. The specificity of NF-κB DNA-binding activity was confirmed by supershift assays (Fig. 4C). Retinoblastoma protein level served as nuclear protein loading control. These data also provide proof of principle and suggest that I3C could be an effective antitumor agent in an animal model of breast cancer bone metastasis, which is mediated by inactivation of NF-κB DNA-binding activity (27, 29). The inactivation of NF-κB may decrease the expression of NF-κB downstream genes, such as CXCR4 and Bcl-2 proteins with concomitant increase in the proapoptotic protein Bax in addition to the alterations in the expression of genes which are involved in the osteolytic and apoptotic processes.

Effect of I3C on the Expression of Bcl-2, Bax, CXCR4, and MMP-9

The effect of CXCR4 expression in tumor tissue (tissue randomly selected from control and treatment groups) was studied by Western blot analysis, and we found a significant down-regulation in the expression of CXCR4 and MMP-9 in tumors of the I3C-treated group (Fig. 5B, *lane 2*) compared with the untreated group (Fig. 5B, *lane 1*). These *in vivo* results were similar to our *in vitro* findings (Fig. 5A, *lanes 2* and *3*). It is known that CXCR4 protein family significantly increases the viability of CD34(+) T-cell precursors by modulating the expression of *Bcl-2* and *Bax* genes and consequently stimulating the proliferation of CD34(+) thymic precursor cells (48). We found that I3C caused a decrease in the expression of Bcl-2 and an increase in the expression of Bax in I3C-treated tumors (Fig. 5B) and MDA-MB-231-cells (Fig. 5A). These results are consistent with our previously published *in vitro* data on Bax and Bcl-2 expression in cells treated with I3C (24, 25). Moreover, recent evidence indicates that deregulation of MMP expression contributes to invasion, metastasis, and tumor angiogenesis (49–55). For example, overexpression of MMP-2 and MMP-9 has been reported to

be positively associated with the progression of human cancers (49–58). Our present results suggest that I3C can inhibit metastasis of breast cancer cells mediated by the inhibition of MMP-9 expression. These results also provide evidence in support of our hypothesis, implicating the role of CXCR4 in metastatic tumor cells by controlling tumor cell migration. Remarkably, we show that CXCR4 may protect tumor cells by reducing apoptotic processes, resulting in increased tumor cell growth and viability. This protective effect involves both the down-regulation of the proapoptotic Bax protein and the up-regulation of the antiapoptotic Bcl-2 protein. The level of Bcl-2 expression was found to be significantly down-regulated in I3C-treated animal tumors and MDA-MB-231 cells (Fig. 5A and B). In contrast, the expression of Bax was found to be significantly up-regulated in I3C-treated animals and MDA-MB-231 cells (Fig. 5A and B). Collectively, our results implicate the role of CXCR4/ NF-κB pathway as a critical event during I3C-induced apoptosis and inhibition of tumor cell proliferation. These preclinical data suggest that I3C could have beneficial effects in patients with breast cancer bone metastasis.

Analysis of CXCR4 and MMP-9 Expression by Immunohistochemistry

Previous studies have shown overexpression of chemokine receptor CXCR4 and/or SDF-1α in metastatic breast cancer cells (6), and these chemokine protein families are also known to activate other metastasis-promoting molecules, such as MMPs, in breast cancer cells (17). Thus, agents that directly block the expression of CXCR-4 could also down-regulate MMP-9 expression, which could also be partly due to inactivation of NF-κB, and this could have great therapeutic potential for treating metastatic breast cancer. To verify the alteration of CXCR4 and MMP-9 by I3C treatment, we conducted immunohistochemical analysis for CXCR4 and
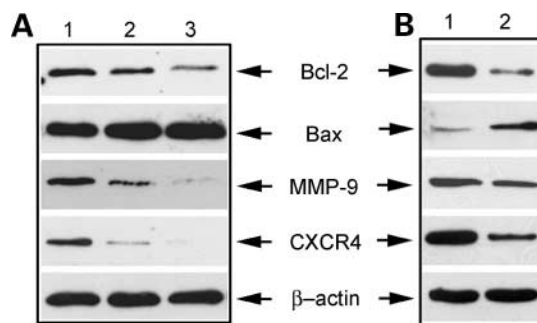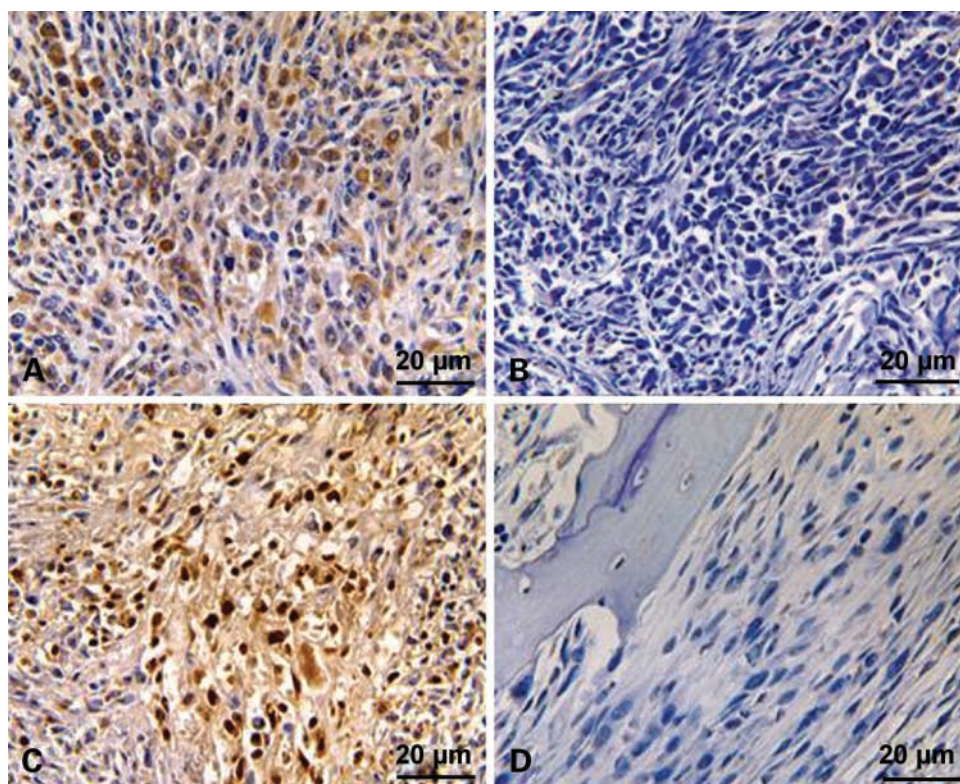

Figure 5. I3C-induced alterations in metastasis-promoting and apoptosis-related genes. **A,** I3C down-regulated metastasis-related protein, such as Bcl-2, Bax, CXCR4, and MMP-9 expression in total cell lysate. Control, MDA-MB-231 cells treated with DMSO; day 3, cells treated with 60 or 100 μmol/L I3C (*lanes 2* and *3*) for 72 h. Whole-cell lysates were prepared and proteins were subjected to Western blot analysis. **B,** Western blot analysis was done on randomly selected frozen tumor tissues obtained from each treatment group of animals. Group 1 (*lane 1*, control animal; *lane 2*, animal received I3C). Results from Western blot analysis showed that the levels of Bcl-2, Bax, CXCR4, and MMP-9 were significantly down-regulated in I3C-treated MDA-MB-231 cells and in animal tumors compared with control group.

Figure 6. Immunohistochemical staining for CXCR4 and MMP-9 in I3C-treated and untreated SCID-hu model and animal tumors done on randomly selected tumor tissues. Tumor cells in untreated control group show intensive staining of CXCR4 (**A**) and MMP-9 (**C**). In contrast, tumor cells in I3C-treated SCID-hu mice show much weaker staining of CXCR4 (**B**) and MMP-9 (**D**). Results from immunohistochemical staining showed that the expression of CXCR4 and MMP-9 was significantly decreased in MDA-MB-231 bone tumors in SCID-hu mice receiving the I3C-containing diet.

MMP-9 protein. The expression of CXCR4 (Fig. 6, *top*) and MMP-9 (Fig. 6, *bottom*), two important molecules of tumor cell survival and metastasis that are downstream of NF-κB, was significantly decreased in MDA-MB-231 bone tumors in SCID-hu mice receiving the I3C (Fig. 6B and D) compared with control (Fig. 6A and C). Overall, our results suggest that the inactivation of NF-κB may indeed reduce the levels of CXCR4 and MMP-9 in the tumor microenvironment resulting in antitumor activity of I3C in our experimental model of breast cancer bone metastasis.

Regulation of the Expression and Activity of MMP-9 by I3C

Treatment with I3C showed down-regulation of MMP-9 by Western blot analysis. Furthermore, we found that I3C significantly inhibited the activity of MMP-9 in conditioned medium in MDA-MB-231 cell culture (Fig. 7A). Together, these results clearly suggest that I3C down-regulates MMP-9; thus, I3C could enhance the antitumor and antimetastatic activity in MDA-MB-231 breast cancer cells. To further support the role of MMP in breast cancer metastasis, we conducted cell invasion assay.

I3C Inhibits Cancer Cell Invasion

It has been well known that MMP-9 is an important molecule involved in cancer cell invasion and metastasis. Because I3C inhibited the expression and activity of MMP-9, we tested the effects of I3C on cancer cell invasion. We found that I3C inhibited invasion of MDA-MB-231 cells through Matrigel matrix membrane compared with control (Fig. 7B and C).

Discussion

The importance of this study lies in the use of a SCID-hu mouse model system that resembles human disease and may also be more relevant to clinical breast cancer than other animal models. Typical osteolytic bone metastasis of MDA-MB-231 cells in a SCID-hu model showed continuous osteolytic and invasive processes resulting in the loss of the bone structure and increased tumor growth, which are believed to be associated with activation of CXCR4/NF-κB signaling pathways (6, 17), similar to those observed in many human breast cancers (6, 17, 59). Our present observations are also in direct agreement with reports showing a significant elevation of CXCR4 in models of metastatic breast cancer with immunodeficient mice (60). Thus, our SCID-hu animal model of breast cancer bone metastasis has offered us an experimental model, in which we have tested the effects of I3C as a chemopreventive or therapeutic agent against breast cancer.

I3C has been shown to target multiple pathways of tumorigenesis, including proliferation, apoptosis, angiogenesis, invasion, and tumor-induced immunosuppression in various breast tumor cell lines (23–27, 29, 38–43, 61–64). Several studies have suggested that chemokine receptor CXCR4 is overexpressed in metastatic breast cancer cells (6). However, no reports exist in the literature elaborating how I3C inhibits CXCR4, a metastatic promoting molecule *in vivo* model of breast cancer cells. In the current report, we show, for the first time, that I3C is an effective agent in the inhibition of cellular growth of breast
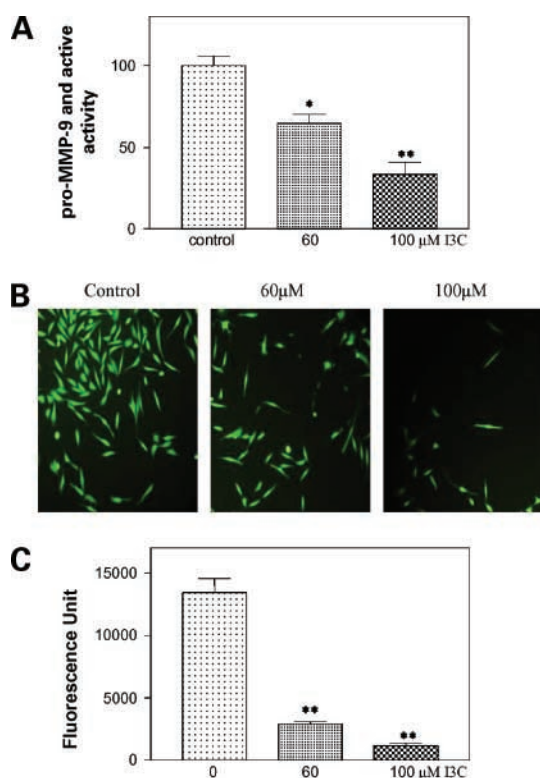
Figure 7. **A,** MMP-9 expression was down-regulated by I3C. MMP-9 activity assay showed that MMP-9 was down-regulated by I3C in the conditioned medium of MDA-MB-231 breast cancer cells. **B,** I3C induced inhibition of MDA-MB-231 cell invasion. Invasion assay showed that I3C significantly inhibited the invasion of MDA-MB-231 cells through Matrigel matrix membrane. **C,** value of fluorescence from the invaded MDA-MB-231 breast cancer cells. The value indicates the comparative amount of invaded MDA-MB-231 breast cancer cells. *, $P < 0.05$; **, $P < 0.01$.

cancer in a bone environment using an animal model of experimental breast cancer bone metastasis. The antitumor activity of I3C was regulated by the inhibition of CXCR4, which is known to regulate the organ-specific trafficking and invasion of metastatic tumor cells mediated by inactivation of NF-κB.

Chemokines and chemokine receptors are believed to play important roles in metastatic breast cancer (6, 59). The most common sites of breast cancer metastases include the lung, liver, lymph node, and bone, in which CXCR4 was found to be highly expressed (6). Moreover, NF-κB, a key transcription factor, may regulate the expression and function of CXCR4, which in turn may activate other metastasis-promoting molecules, such as MMP-9 in breast cancer cells (17). A recent study also showed that the promoter region of CXCR4 has several NF-κB-binding sites, suggesting that there may be a cross-talk between NF-κB and CXCR4 (17). In models of metastatic breast cancer, the administration of neutralizing antibodies or peptide antagonists of CXCR4 substantially reduced lung metastases (6, 65). CXCR4 expression was found to be up-regulated in murine lung metastases in a

NF-κB-dependent fashion (17), again suggesting that CXCR4 signaling is an important determinant of metastatic breast cancer. Moreover, a significant correlation between the relative expression levels of CXCR4 and the extent of lymph node metastases was found in invasive ductal carcinomas of the breast in humans. The expression of CXCR4 was also found to be increased in invasive ductal carcinoma specimens compared with ductal carcinoma *in situ* and normal breast epithelium. CXCR4 expression by normal breast stromal cells adjacent to malignant cells was also increased (66). We anticipated that CXCR4 in the tumor microenvironment may function to promote breast cancer proliferation, migration, and invasion, and our current data suggest that I3C could interrupt this signaling pathway, resulting in tumor growth inhibition of breast cancer bone metastasis.

Our present data recapitulate recent *in vitro* results in breast cancer cell lines, showing that I3C induces apoptosis by blocking NF-κB activation (27, 29). Moreover, NF-κB, a key transcription factor, may regulate the expression and function of CXCR4 and activate other metastasis-promoting molecules (uPA and MMPs) in breast cancer cells (17). Decreased expression of CXCR4 was associated with decreased expression of NF-κB, which in turn reduced the levels of MMP-9 in tumors treated with I3C. This could be one of the mechanism(s) underlying enhanced tumor cell apoptosis and reduced tumor cell proliferation *in vivo*. Taken together, our results suggest multiple functions of NF-κB in the growth, migration, and organ-specific metastasis of breast cancer cells, which, in part, appear to be mediated through the induction of CXCR4. Moreover, the CXCR4/NF-κB pathways activated MMP-9 expression in breast cancer bone metastasis and were also abrogated by I3C, thus suggesting that our model could be useful to fully evaluate the role of CXCR4/NF-κB pathways *in vivo* as well as its mechanistic role in the inhibition of tumor cell invasion and metastasis (Fig. 8).

Several other potential mechanism(s) could also explain the regulation of CXCR4 associated with breast cancer metastasis (Fig. 8). One potential mechanism that has been associated with CXCR4-related inhibition of apoptosis is that CXCR4 reduces the apoptotic rate by increasing the level Bcl-2 expression and decreasing the level of Bax expression (48). Our *in vivo* and *in vitro* data support this concept because inhibiting NF-κB production by targeting CXCR4 activity in the SCID-hu tumors led to a decrease in Bcl-2 protein levels, a concomitant increase in the proapoptotic protein Bax, and decreased MMP-9 expression. These results are consistent with our previously published *in vitro* data on Bax/Bcl-2 expression (24, 25) and provide support for our hypothesis, implying the role of CXCR4 in metastatic tumor cells, suggesting that I3C could be beneficial in patients with breast cancer bone metastasis.

In addition to these mechanism(s), MMP-9 has also been reported to be involved in cancer invasion and metastasis (52, 53, 55). Several studies have shown that MMPs play prominent roles in metastasis (49–53, 55). MMP-9 has been
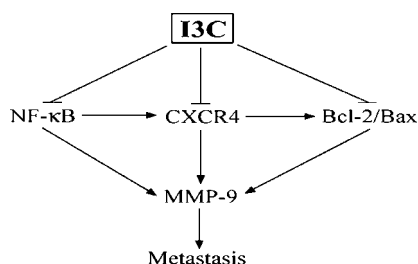
Figure 8. Hypothetical diagram showing the role of CXCR4, MMP-9, and/or other genes in breast cancer cells in a metastatic model and further showing that these molecules could be inhibited by I3C mediated by the inactivation of the NF-κB pathway.

implicated in metastasis because of its role in the degradation of basement membrane collagen. In addition, MMP activity is known to play a role in both normal and cancer-induced bone remodeling. It has been reported that NF-κB and MMPs are involved in the processes of tumor invasion and metastasis (67). In this study, we found that I3C inhibited the expression, secretion, and activation of MMP-9, suggesting that I3C could prevent bone matrix degradation and reduce breast cancer cell growth in human bone implanted in SCID mice. The down-regulation of MMP-9 by I3C could be mediated by the down-regulation of NF-κB whose binding site has been found in the promoter of MMP-9 (67, 68). These results suggest that I3C could promote the antitumor and antimetastasis activities in SCID-hu model of breast cancer bone metastasis partly through the down-regulation of MMP expression (Fig. 8). Because we observed that I3C down-regulated MMP-9, we tested the effects of I3C on the invasion of MDA-MB-231 breast cancer cells and found that I3C inhibited the invasion of MDA-MB-231 breast cancer cells. These results corresponded with MMP-9 data, showing that I3C could inhibit cancer cell invasion partly through down-regulation of MMP-9.

In summary, I3C treatment may exert its antiproliferative, antiangiogenic, and proapoptotic effects by decreasing CXCR4 and MMP-9 expression, which was associated via the down-regulation of the NF-κB pathway. In this report, we have shown that reduced expression of CXCR4 by I3C limits cellular growth of breast cancer cells in a bone environment and prevents breast cancer bone metastasis. These results further extend the potential therapeutic application of I3C for metastatic breast cancer.

References

1. Liotta LA. An attractive force in metastasis. Nature 2001;410:24 – 5.

2. Liotta LA, Kohn EC. The microenvironment of the tumour-host interface. Nature 2001;411:375 – 9.

3. Chambers AF, Matrisian LM. Changing views of the role of matrix metalloproteinases in metastasis. J Natl Cancer Inst 1997;89:1260 – 70.

4. Edward KL, Jeffery RM. Estrogen-induced mitogenesis of MCF-7 cells

5. Coleman RE, Rubens RD. The clinical course of bone metastases from breast cancer. Br J Cancer 1987;55:61 – 6.

6. Muller A, Homey B, Soto H, et al. Involvement of chemokine receptors in breast cancer metastasis. Nature 2001;410:50 – 6.

7. Chinni SR, Sivalogan S, Dong Z, et al. CXCL12/CXCR4 signaling activates Akt-1 and MMP-9 expression in prostate cancer cells: the role of bone microenvironment-associated CXCL12. The Prostate 2006;66: 32 – 48.

8. Han YP, Hughes MW, Nien YD, et al. IL-8-stimulated expression of urokinase-type plasminogen activator in human skin and human epidermal cells. J Surg Res 2002;106:328 – 34.

9. Lane WJ, Dias S, Hattori K, et al. Stromal-derived factor 1-induced megakaryocyte migration and platelet production is dependent on matrix metalloproteinases. Blood 2000;96:4152 – 9.

10. Moore MA. The role of chemoattraction in cancer metastases. Bioessays 2001;23:674 – 6.

11. Murphy P. Chemokines and the molecular basis of cancer metastasis. N Engl J Med 2001;345:833 – 5.

12. Nakshatri H, Goulet RJ, Jr. NF-κB and breast cancer. Curr Probl Cancer 2002;26:282 – 309.

13. Taichman RS, Cooper C, Keller ET, et al. Use of the stromal cell-derived factor-1/CXCR4 pathway in prostate cancer metastasis to bone. Cancer Res 2002;62:1832 – 7.

14. Pallares J, Martinez-Guitarte JL, Dolcet X, et al. Abnormalities in the NF-κB family and related proteins in endometrial carcinoma. J Pathol 2004;204:569 – 77.

15. Wu JT, Kral JG. The NF-κB/IκB signaling system: a molecular target in breast cancer therapy. J Surg Res 2005;123:158 – 69.

16. Ganju RK, Brubaker SA, Meyer J, et al. The α-chemokine, stromal cell-derived factor-1α, binds to the transmembrane G-protein-coupled CXCR-4 receptor and activates multiple signal transduction pathways. J Biol Chem 1998;273:23169 – 75.

17. Helbig G, Christopherson KW II, Bhat-Nakshatri P, et al. NF-κB promotes breast cancer cell migration and metastasis by inducing the expression of the chemokine receptor CXCR4. J Biol Chem 2003;278: 21631 – 8.

18. Kukreja P, Abdel-Mageed AB, Mondal D, et al. Up-regulation of CXCR4 expression in PC-3 cells by stromal-derived factor-1α (CXCL12) increases endothelial adhesion and transendothelial migration: role of MEK/ERK signaling pathway-dependent NF-κB activation. Cancer Res 2005;65:9891 – 8.

19. Karin M, Cao Y, Greten FR, et al. NF-κB in cancer: from innocent bystander to major culprit. Nat Rev Cancer 2002;2:301 – 10.

20. Chinni SR, Li Y, Upadhyay S, et al. Indole-3-carbinol (I3C) induced cell growth inhibition, G$_1$ cell cycle arrest and apoptosis in prostate cancer cells. Oncogene 2001;20:2927 – 36.

21. Chinni SR, Sarkar FH. Akt inactivation is a key event in indole-3-carbinol-induced apoptosis in PC-3 cells. Clin Cancer Res 2002;8:1228 – 36.

22. Li Y, Chinni SR, Sarkar FH. Selective growth regulatory and pro-apoptotic effects of DIM is mediated by AKT and NF-κB pathways in prostate cancer cells. Front Biosci 2005;10:236 – 43.

23. Li Y, Li X, Sarkar FH. Gene expression profiles of I3C- and DIM-treated PC3 human prostate cancer cells determined by cDNA microarray analysis. J Nutr 2003;133:1011 – 9.

24. Rahman KM, Aranha O, Glazyrin A, et al. Translocation of Bax to mitochondria induces apoptotic cell death in indole-3-carbinol (I3C) treated breast cancer cells. Oncogene 2000;19:5764 – 71.

25. Rahman KM, Aranha O, Sarkar FH. Indole-3-carbinol (I3C) induces apoptosis in tumorigenic but not in nontumorigenic breast epithelial cells. Nutr Cancer 2003;45:101 – 12.

26. Rahman KM, Sarkar FH. Steroid hormone mimics: molecular mechanisms of cell growth and apoptosis in normal and malignant mammary epithelial cells. J Steroid Biochem Mol Biol 2002;80:191 – 201.

27. Rahman KM, Li Y, Sarkar F. Inactivation of Akt and NF-κB plays important roles during I3C-induced apoptosis in breast cancer cells. Nutr Cancer 2004;48:84 – 94.

28. Rahman KM, Li Y, Wang Z, et al. Gene expression profiling revealed

does not require the induction of mitogen-activated protein kinase activity. J Steroid Biochem Mol Biol 2000;75:11 – 20.

survivin as a target of DIM-induced cell growth inhibition and apoptosis in breast cancer cells. Cancer Res 2006;66:4952 – 60.

29. Rahman KM, Sarkar FH. Inhibition of nuclear translocation of nuclear factor-κB contributes to 3,3′-diindolylmethane-induced apoptosis in breast cancer cells. Cancer Res 2005;65:364 – 71.

30. Kim YS, Milner JA. Targets for indole-3-carbinol in cancer prevention. J Nutr Biochem 2005;16:65 – 73.

31. Meng F, Liu L, Chin PC, et al. Akt is a downstream target of NF-κB. J Biol Chem 2002;277:29674 – 80.

32. Basu GD, Pathangey LB, Tinder TL, et al. Cyclooxygenase-2 inhibitor induces apoptosis in breast cancer cells in an *in vivo* model of spontaneous metastatic breast cancer. Mol Cancer Res 2004;2:632 – 42.

33. Eckhardt BL, Parker BS, van Laar RK, et al. Genomic analysis of a spontaneous model of breast cancer metastasis to bone reveals a role for the extracellular matrix. Mol Cancer Res 2005;3:1 – 13.

34. Nemeth JA, Harb JF, Barroso U, Jr., et al. Severe combined immunodeficient-hu model of human prostate cancer metastasis to human bone. Cancer Res 1999;59:1987 – 93.

35. Hillman GG, Wang Y, Kucuk O, et al. Genistein potentiates inhibition of tumor growth by radiation in a prostate cancer orthotopic model. Mol Cancer Ther 2004;3:1271 – 9.

36. Strickley RG. Solubilizing excipients in oral and injectable formulations. Pharm Res 2004;21:201 – 30.

37. Chaturvedi MM, Mukhopadhyay A, Aggarwal BB. Assay for redox-sensitive transcription factor. Methods Enzymol 2000;319:585 – 602.

38. Aggarwal BB, Ichikawa H. Molecular targets and anticancer potential of indole-3-carbinol and its derivatives. Cell Cycle 2005;4:1201 – 15.

39. Brandi G, Paiardini M, Cervasi B, et al. A new indole-3-carbinol tetrameric derivative inhibits cyclin-dependent kinase 6 expression and induces G$_1$ cell cycle arrest in both estrogen-dependent and estrogen-independent breast cancer cell lines. Cancer Res 2003;63:4028 – 36.

40. Riby JE, Chang GH, Firestone GL, et al. Ligand-independent activation of estrogen receptor function by 3,3′-diindolylmethane in human breast cancer cells. Biochem Pharmacol 2000;60:167 – 77.

41. Riby JE, Feng C, Chang YC, et al. The major cyclic trimeric product of indole-3-carbinol is a strong agonist of the estrogen receptor signaling pathway. Biochemistry 2000;39:910 – 8.

42. Shertzer HG. Indole-3-carbinol protects against covalent binding of benzo[*a*]pyrene and *N*-nitrosodimethylamine metabolites to mouse liver macromolecules. Chem Biol Interact 1984;48:81 – 90.

43. Shertzer HG, Senft AP. The micronutrient indole-3-carbinol: implications for disease and chemoprevention. Drug Metabol Drug Interact 2000; 17:159 – 88.

44. Firestone GL, Bjeldanes LF. Indole-3-carbinol and 3-3′-diindolylmethane antiproliferative signaling pathways control cell-cycle gene transcription in human breast cancer cells by regulating promoter-Sp1 transcription factor interactions. J Nutr 2003;133:2448 – 55S.

45. Meng Q, Goldberg ID, Rosen EM, et al. Inhibitory effects of Indole-3-carbinol on invasion and migration in human breast cancer cells. Breast Cancer Res Treat 2000;63:147 – 52.

46. Wu HT, Lin SH, Chen YH. Inhibition of cell proliferation and *in vitro* markers of angiogenesis by indole-3-carbinol, a major indole metabolite present in cruciferous vegetables. J Agric Food Chem 2005;53:5164 – 9.

47. Nemeth JA, Yousif R, Herzog M, et al. Matrix metalloproteinase activity, bone matrix turnover, and tumor cell proliferation in prostate cancer bone metastasis. J Natl Cancer Inst 2002;94:17 – 25.

48. Hernandez-Lopez C, Varas A, Sacedon R, et al. Stromal cell-derived factor 1/CXCR4 signaling is critical for early human T-cell development. Blood 2002;99:546 – 54.

49. Curran S, Murray GI. Matrix metalloproteinases: molecular aspects of their roles in tumour invasion and metastasis. Eur J Cancer 2000;36: 1621 – 30.

50. Dong Z, Bonfil RD, Chinni S, et al. Matrix metalloproteinase activity and osteoclasts in experimental prostate cancer bone metastasis tissue. Am J Pathol 2005;166:1173 – 86.

51. John A, Tuszynski G. The role of matrix metalloproteinases in tumor angiogenesis and tumor metastasis. Pathol Oncol Res 2001;7:14 – 23.

52. Li Y, Che M, Bhagat S, et al. Regulation of gene expression and inhibition of experimental prostate cancer bone metastasis by dietary genistein. Neoplasia 2004;6:354 – 63.

53. Li Y, Kucuk O, Hussain M, et al. Antitumor and antimetastatic activities of docetaxel are enhanced by genistein through regulation of osteoprotegerin/receptor activator of nuclear factor-κB (RANK)/RANK ligand/MMP-9 signaling in prostate cancer. Cancer Res 2006;66:4816 – 25.

54. McCawley LJ, Matrisian LM. Matrix metalloproteinases: they're not just for matrix anymore! Curr Opin Cell Biol 2001;13:534 – 40.

55. Przybylowska K, Kluczna A, Zadrozny M, et al. Polymorphisms of the promoter regions of matrix metalloproteinases genes MMP-1 and MMP-9 in breast cancer. Breast Cancer Res Treat 2006;95:65 – 72.

56. Sato H, Takino T, Okada Y, et al. A matrix metalloproteinase expressed on the surface of invasive tumour cells. Nature 1994;370:61 – 5.

57. Waas ET, Lomme RM, DeGroot J, et al. Tissue levels of active matrix metalloproteinase-2 and -9 in colorectal cancer. Br J Cancer 2002;86: 1876 – 83.

58. Wang M, Wang T, Liu S, et al. The expression of matrix metalloproteinase-2 and -9 in human gliomas of different pathological grades. Brain Tumor Pathol 2003;20:65 – 72.

59. Goldberg-Bittman L, Neumark E, Sagi-Assif O, et al. The expression of the chemokine receptor CXCR3 and its ligand, CXCL10, in human breast adenocarcinoma cell lines. Immunol Lett 2004;92:171 – 8.

60. Smith MC, Luker KE, Garbow JR, et al. CXCR4 regulates growth of both primary and metastatic breast cancer. Cancer Res 2004;64: 8604 – 12.

61. Cover CM, Hsieh SJ, Tran SH, et al. Indole-3-carbinol inhibits the expression of cyclin-dependent kinase-6 and induces a G$_1$ cell cycle arrest of human breast cancer cells independent of estrogen receptor signaling. J Biol Chem 1998;273:3838 – 47.

62. Garcia HH, Brar GA, Nguyen DH, et al. Indole-3-carbinol (I3C) inhibits cyclin-dependent kinase-2 function in human breast cancer cells by regulating the size distribution, associated cyclin E forms, and subcellular localization of the CDK2 protein complex. J Biol Chem 2005;280: 8756 – 64.

63. Herraiz T, Galisteo J. Endogenous and dietary indoles: a class of antioxidants and radical scavengers in the ABTS assay. Free Radic Res 2004;38:323 – 31.

64. Manson MM, Farmer PB, Gescher A, et al. Innovative agents in cancer prevention. Recent Results Cancer Res 2005;166:257 – 75.

65. Liang Z, Wu T, Lou H, et al. Inhibition of breast cancer metastasis by selective synthetic polypeptide against CXCR4. Cancer Res 2004;64: 4302 – 8.

66. Allinen M, Beroukhim R, Cai L, et al. Molecular characterization of the tumor microenvironment in breast cancer. Cancer Cell 2004;6:17 – 32.

67. Ricca A, Biroccio A, Del Bufalo D, et al. bcl-2 over-expression enhances NF-κB activity and induces mmp-9 transcription in human MCF7(ADR) breast-cancer cells. Int J Cancer 2000;86:188 – 96.

68. Takada Y, Andreeff M, Aggarwal BB. Indole-3-carbinol suppresses NF-κB and IκBα kinase activation, causing inhibition of expression of NF-κB-regulated antiapoptotic and metastatic gene products and enhancement of apoptosis in myeloid and leukemia cells. Blood 2005;106:641 – 9.